Evaluation of heating performances of different ventilation methods in an office

Article

Accepted Version

Central Archive at the University of Reading

Reading's research outputs online

Evaluation of heating performances of different ventilation methods in an office

Teng Li[1,2], Emmanuel A. Essah[3], Yuxin Wu[4], Chunhui Liao[5], and Yong Cheng[1,2*]

[1]Joint International Research Laboratory of Green Buildings and Built Environments, Ministry of Education, Chongqing University, Chongqing, China

[2]National Centre for International Research of Low-carbon and Green Buildings, Ministry of Science & Technology, Chongqing University, Chongqing, China

[3]School of Construction Management and Engineering, The University of Reading, United Kingdom

[4]School of Civil Engineering and Architecture, Zhejiang Sci-Tech University, Zhejiang, China

[5]Instiue for Health and Environment, Chongqing University of Science and Technology, Chongqing, China

*Corresponding author. Tel.: +86 2365123213; E-mail: yongcheng6@cqu.edu.cn

ABSTRACT

In this study, twelve cases were investigated in an office-layout room using experiments and computational fluid dynamics (CFD) simulations. The heating performances of four ventilation methods (*i.e.*, Mixing Ventilation (MV), Stratum Ventilation (SV), Deflection Ventilation (DeV) and Impinging Jet Ventilation (IJV)) were comprehensively compared by various evaluation indexes (*i.e.*, predicted mean vote (PMV), draught rate (DR), vertical air temperature difference ($\triangle$T), air diffusion performance index (ADPI), energy utilization coefficient (EUC), air change efficiency (ACE) and contaminant removal efficiency (CRE)). Better thermal comfort was found in rooms heated by SV and DeV. The PMV, DR and $\triangle$T under SV and DeV complied with Category B of ISO 7730:2005, and the ADPI was in full compliance with the stipulation of ANSI/ASHRAE 113-2022. For the energy-saving characteristic, the targeted-occupied-zone ventilation methods (*i.e.*, SV, DeV and IJV) can effectively deliver warm air to the occupied zone, with the EUC values higher than unity and thus providing a good potential for energy saving. SV and IJV showed slightly higher ACEs at the breathing zone. The contaminant removal effectiveness of SV, DeV and IJV was comparable. Under

the combined influence of occupant thermal plumes and locations of exhausts, MV showed a high CRE. However, the CRE under MV decreased significantly when the exhausts were not above occupants. In the case of supply air parameters in this study, the entropy weight method indicated that DeV and SV had a better overall performance for winter heating, followed by IJV and then MV.

Keywords: ventilation method; winter heating; thermal comfort; inhaled air quality; energy saving; overall performance

Introduction

The quality of an indoor environment can ensure the health of occupants and improve their work efficiencies.[1, 2] Ventilation is regarded as an effective method to control indoor air parameters and dilute and/or remove indoor pollutants.[3] Nevertheless, ventilation methods have a great influence on the ventilation effect. Work efficiency and air quality can be optimized with a low energy cost by using an appropriate ventilation method.[4] Therefore, ventilation methods are essential to achieve the goal of low carbon emission, satisfactory thermal comfort and quality inhaled air.[5]

Mixing Ventilation (MV) was applied to various types of building spaces with a long history of development.[3] Some studies have been carried out to improve the heating performance of MV.[4, 6, 7] At the same time, some advanced ventilation methods have been proposed. Amongst them, Stratum Ventilation (SV), Deflection Ventilation (DeV) and Impinging Jet Ventilation (IJV) are three typical novel methods.

In a review of the characteristics of various ventilation methods,[8] the non-uniform ventilation methods, such as SV and IJV, were shown to perform better in improving thermal comfort and indoor air quality as compared with the typical uniform ventilation method during cooling season. In the room served by SV, the fresh air can be delivered directly into the occupied zone by locating the supply terminals at the side wall slightly above the head level of occupants, which can create a comfortable indoor environment with a low energy cost.[9] Compared with traditional MV and Displacement Ventilation (DV), in summer, SV can provide satisfactory thermal comfort and higher inhaled air quality, as well as energy efficiency.[10, 11, 12] For winter heating, the airflow is affected by positive thermal buoyancy, which can be different from summer in the room served by SV.[13] With the appropriate supply air temperature and velocity, SV can warm the occupied zone efficiently to achieve satisfactory thermal comfort[13, 14] and quality inhaled air.[15] In the case of DeV, the supply air jet is innovatively guided using a deflector to effectively enter the occupied zone. DeV could realize

better thermal comfort with a small temperature difference between the head and ankle level compared with conventional ventilation methods for summer cooling.[16] Through investigating the airflow field of DeV in summer and winter, the results showed that DeV could create a clean and comfortable occupied zone with a lower supply airflow rate.[17] DeV had a high particle removal efficiency, which can provide the occupants with a clean breathing zone in heating mode.[18] For IJV, in the lower occupied zone, a fresh air layer was formed after the collision between the supply air jet and the floor.[19] IJV had the potential to be applied for both winter and summer scenarios.[20, 21] During summer cooling, IJV can provide satisfactory thermal comfort and indoor air quality.[19] Compared with the traditional MV system, IJV can distribute warm air to the occupied zone more effectively, and the total heating energy efficiency was higher in heating mode.[22]

As mentioned above, there are significant differences in the performances of different ventilation methods,[16, 22] as well as differences in the heating and cooling performances of the same ventilation method due to the influence of thermal buoyancy.[13, 23] Some previous research suggested that people should have a better consideration regarding the indoor environment in winter.[18, 22, 24] However, for some advanced ventilation methods, a comprehensive comparison of thermal comfort, inhaled air quality and energy-saving characteristics in heating mode is lacking.

In this study, experiments and numerical simulations were carried out for an experimental office. With different supply air parameters, four ventilation methods were compared comprehensively on thermal environment, inhaled air quality and energy-saving characteristics. Seven different evaluation indexes were used to evaluate the heating performances of ventilation methods, and the entropy-weight method was used for overall performance analysis. The findings of this study can provide relevant design information for ventilation applications in winter where heating is required.

Methodology

Description of the geometry

The office model has the dimensions of 5.85 m (X, length) × 5.06 m (Y, width) × 2.80 m (Z, height), as shown in Figure 1. It consists of four walls, a window, a desk, two thermal manikins and six fluorescent lamps. The window-to-wall ratio is 0.26. In this study, since we focused on the global airflow conditions and ventilation performances, the sedentary occupant was rationally simplified as a hexahedron (0.4 m (X) × 0.25 m (Y) × 1.2 m (Z)).[10] In order to simulate the heat of the human body, a light bulb of 100 W was installed inside each thermal manikin. Six lamps were fixed on the ceiling

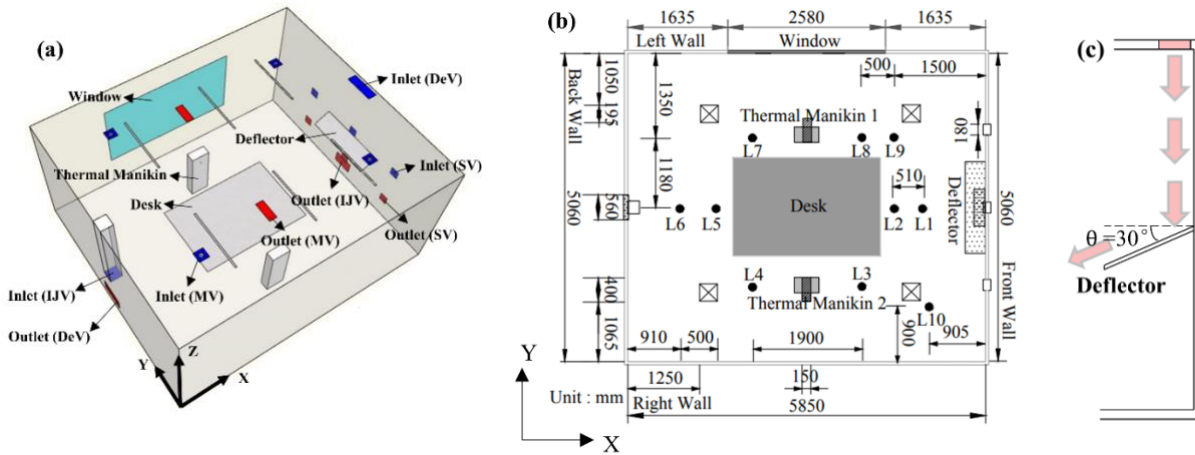to illuminate the office. The generated heat of each lamp was 23 W.

Figure 1. Layout of the office, (a) Physical model, (b) Schematic plan, (c) Deflection angle of DeV.
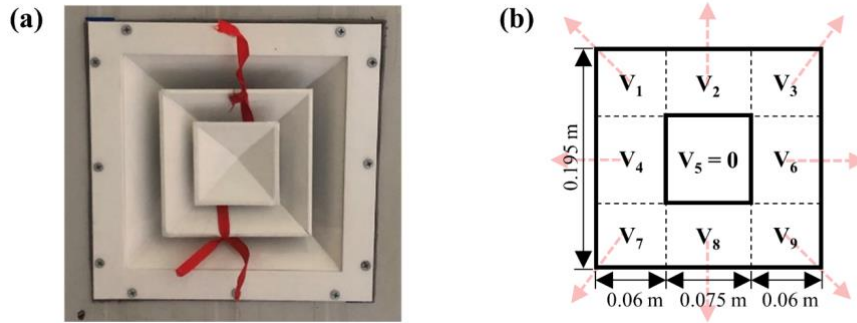

Figure 2. (a) Square ceiling diffuser in the test chamber, (b) Nine-point model of square diffuser in CFD simulation.

Figure 1 shows the typical layout of the office ventilated by MV, SV, DeV and IJV. For MV, the supply inlets were four square ceiling diffusers (0.195 m × 0.195 m), which can be seen in Figure 2. Two exhaust outlets each with the dimensions of 0.2 m × 0.4 m, were symmetrically installed on the ceiling. For SV, it was achieved by three double grille diffusers and three exhaust outlets each with the dimensions of 0.18 m × 0.18 m. The inlets and outlets of SV were arranged at heights of 1.3 and 0.4 m above the floor, respectively, and the inclination angle of supply inlets was 30° downward in winter. For DeV, the warm air was delivered vertically downward through the inlet (0.58 m × 0.184 m), located on the ceiling and close to the front wall. The deflector (1.5 m × 0.4 m) was fixed on the wall at a height of 1.3 m above the floor. The deflection angle of the deflector under DeV was set as 30° downward, as shown in Figure 1(c). The air was exhausted through an opposite-wall-based outlet (0.56 m × 0.26 m) at a height of 0.21 m above the floor. For IJV, the supply air inlet was a square

nozzle (0.2 m × 0.2 m), which was located at a height of 1.0 m above the floor. The exhaust outlet was located on the opposite wall, which had a similar size as that of DeV. For all cases, the layouts of inlets and outlets are similar to previous research.[17, 25, 26, 27]

Studied cases

A total of twelve cases were designed to be investigated experimentally and numerically, including four ventilation methods (*i.e.*, MV, SV, DeV and IJV), two nominal supply air temperatures (*i.e.*, 24 and 26°C) and two ventilation rates (*i.e.*, 322 and 496 m^3/h, corresponding to 3.88 and 5.98 air changes per hour, respectively). To make a comparison, the designed supply air parameters were typical for the four ventilation methods in winter.[26] In this study, the initial Reynolds numbers and Archimedes numbers of these cases were approximately 9,500 – 34,000 and 0.006 – 0.07, respectively. To compare the heating performances of different ventilation methods, experimental measurements and numerical simulation methods were used concurrently. The experiments were carried out to characterize the distributions of air parameters and to compare the thermal environments and the energy saving characteristics of ventilation methods. Meanwhile, the experimental data were also used for the validation of numerical simulation. All the cases were simulated by the computational fluid dynamics (CFD) method to reflect the details of indoor flow fields and to compare inhaled air quality. The results of IJV were only derived from CFD simulations, which were validated by experimental data. Table 1 lists details of the information on the studied cases. For all cases, the deviations between the actual measured supply air temperatures (T_s) and the corresponding nominal values were less than 0.5°C, indicating the experimental conditions were well controlled.

Table 1. Information of studied cases.

Case	Ventilation method	Studied method	ACH (h^{-1})	V_s (m/s)	T_s (°C)	T_r (°C)	T_{wall} (°C)	T_{window} (°C)	T_e (°C)	RH (%)	Re	Ar
1	MV	EXP, CFD	3.88	0.69	23.9	20.2	19.2	18.0	21.9	45.4	9,511	0.060
2	MV	EXP, CFD	3.88	0.69	25.8	20.4	19.4	18.3	22.6	42.8	9,396	0.069
3	MV	EXP, CFD	5.98	1.06	25.8	20.8	19.8	18.2	22.8	43.0	14,435	0.032
4	SV	EXP, CFD	3.88	0.92	24.3	20.6	19.6	18.8	20.2	47.1	12,681	0.021
5	SV	EXP, CFD	3.88	0.92	26.1	21.4	20.2	18.7	20.8	46.8	12,528	0.032
6	SV	EXP, CFD	5.98	1.42	26.1	21.9	20.5	18.6	21.7	45.2	19,337	0.016

			ACH	V_s	T_s	T_r	T_{wall}	T_{window}	T_e	RH	Re	Ar
7	DeV	EXP, CFD	3.88	0.84	24.2	19.5	18.0	16.7	18.6	41.4	21,034	0.039
8	DeV	EXP, CFD	3.88	0.84	26.2	20.3	19.0	17.7	19.6	38.7	20,780	0.051
9	DeV	EXP, CFD	5.98	1.29	26.0	21.4	19.6	17.7	20.9	38.7	31,913	0.034
10	IJV	CFD	3.88	1.43	24.0	20.6	19.0	17.0	20.3	40.0	21,901	0.006
11	IJV	CFD	3.88	1.43	26.0	21.2	19.0	17.0	20.8	40.0	21,637	0.009
12	IJV	CFD	5.98	2.21	26.0	21.6	19.0	17.0	21.2	40.0	33,439	0.007

Note: EXP represents experiment; CFD represents computational fluid dynamics; ACH is air changes per hour; V_s is supply air velocity; T_s is measured supply air temperature; T_r is the average air temperature in the occupied zone; T_{wall} is the average interior surface temperature of the walls (the temperature differences between different walls in this study were less than 1°C); T_{window} is the interior surface temperature of the window; T_e is exhaust air temperature; RH is a relative humidity of the room. For IJV, the room's relative humidity was set as 40%.[8] Re is initial Reynolds number, $Re = (V_s \rho \sqrt{Ae})/\mu$, where ρ is air density (kg/m³), Ae is the effective area of supply air inlet (m²), μ is dynamic viscosity (Pa·s); Ar is Archimedes number, $Ar = [g\sqrt{Ae}\,(T_s - T_r)]/[V_s^2(T_r + 273.15)]$, where g is gravitational acceleration, g = 9.81 m/s².

Experimental study

The experiments were carried out in a full scale office-layout chamber (see Figure 1), located in Chongqing, China. The chamber was arranged inside the building room, and the walls and window were internal envelopes. Under each ventilation method, the indoor air pressure was slightly positive, so the impact of cold air infiltration was not considered. The experiments were conducted under three different ventilation methods (*i.e.*, MV, SV and DeV). The ventilation methods in the test chamber can be transformed by switching the valves. To sufficiently characterize the airflow information, ten sampling plumb lines (L1 – L10) were arranged in the testing space (see Figure 1(b)). Five Swema 03+ omnidirectional anemometers were fixed along each sampling line and used to collect the data at five different heights (*i.e.,* 0.1, 0.6, 1.1, 1.7 and 2.4 m above the floor), with a sampling frequency of 5 Hz. The measured value was air speed (*i.e.*, the magnitude of air velocity), but in this study, the term "velocity" was used for simplicity. The varied heights were measured to investigate the air velocity and temperature patterns along the vertical profiles for each ventilation method. The accuracy of the velocity measurement is ± 0.03 m/s ± 3% of readings within the range of 0.05 – 10 m/s, and the error of the measured temperature is ± 0.2°C within the range of 10 – 40°C. The accuracy of the anemometers complies with the recommendations of ANSI/ASHRAE 113-2022.[28] Meanwhile, the temperatures of supply air, exhaust air, and all the walls and window were monitored by automated thermal recorders (WZY-1) with a sampling frequency of 1/60 Hz. The air temperature at the inlet was monitored in real-time to ensure that the temperature fluctuation of the supply airflow

was within 5% of the nominal value. The error of the measured temperature by the WZY-1 recorder was $\pm 0.3°C$ within the range of -20 – 80°C. Additionally, indoor relative humidity was logged by pSENSE II data logger (SenseAir, Sweden). The measurement range was from 0.1% to 99.9% with an accuracy of $\pm 3\%$. Before the formal experiments, all the experimental instruments had been calibrated. Details of each instrument are summarized in Table 2.

Table 2. Specifications of measurement instruments.

Instrument		Parameter	Range	Accuracy	Frequency
WZY-1 recorder		Temperature	-20 – 80°C	$\pm 0.3°C$	1/60 Hz
Swema 03+ omnidirectional anemometers		Temperature	10 – 40°C	$\pm 0.2°C$	5 Hz
		Velocity	0.05 – 10 m/s	± 0.03 m/s $\pm 3\%$ of reading	5 Hz
pSENSE II data logger		Relative humidity	0.1% – 99.9%	$\pm 3\%$	1 Hz
		CO_2 concentration	0 – 9,999 ppm	± 30 ppm	1 Hz

The supply airflow rate was set by regulating the rotation frequency of the fan using an automatic control system. Anemometers were used to measure the supply airflow rates corresponding to the frequency of the fan before the experiments. In addition, the supply air temperatures could be adjusted by an electric heater using the control panel of an air-conditioning system. The air velocity and temperature at the inlet were measured at uniformly distributed multiple points, and the values represented their average values. Before the measurement of each case, the air conditioning system was turned on for at least one hour.[13] A steady airflow field was assumed to be achieved when the monitoring air parameters were statistically steady, and the data started to be collected. However, due to the limited number of anemometers, the air velocity and temperature along one sampling line were measured line by line by shifting the probe holding pole. For each sampling line, the measuring duration was at least 12 min.[13] After each pole shifting, there was at least 10 min lapse between measurements to ensure the air parameters reach a steady state again.[29]

CFD simulation

Numerical details

To understand indoor air distribution characteristics in detail and compare the inhaled air qualities under different ventilation methods, the validated CFD simulations were carried out. This study used ICEM, a component within the ANSYS CFD software, to construct the 3-D model and generate grids. FLUENT, the numerical solver component of ANSYS was used to carry out the simulation calculations.

The geometric model developed within ANSYS was the same as that illustrated in Figure 1. The mouth of each occupant was modelled at 0.9 m above the floor, with the size of 0.01 m × 0.02 m.[30] CO_2 was assumed to be exhaled from mouths with a constant rate of 0.01872 m^3/h and a constant temperature of 35°C, representing an average sized adult engaging in office work with a metabolic rate of 1.2 met.[21] The supply air inlets were defined as velocity inlet by setting the magnitude and direction of velocity. The corresponding magnitudes and temperatures can be found in Table 1. The square ceiling diffusers were modelled for MV using a nine-point method.[31] The established supply air inlet model is shown in Figure 2(b). All the outlets were set as "outflow" boundary conditions. The temperatures of walls and windows were the measured values during experiments (see Table 1). The desk, floor and ceiling were treated as adiabatic. The heat fluxes of 639 and 62.5 W/m^2 were defined for the lamps and thermal manikins, respectively.

The standard k-ε turbulence model was employed to solve the airflow,[15, 32] which was considered a trade-off between the prediction accuracy and computational cost. The species transport model was used to predict the contaminant dispersion. The general governing equation of the model for steady flow is given as Equation (1). For all cases, the non-dimensional distances of walls (y^+) were higher than 11.23, and the standard wall function was used for near-wall treatment.[15] All the surfaces in the office were set as non-slipped. The SIMPLE algorithm was used to solve the airflow field, and the second-order upwind scheme was selected. Boussinesq model was employed to consider buoyancy effect. Discrete Ordinates (DO) radiation model was employed to calculate the radiation heat transfer among the solid surfaces. The solution was judged to be convergent when the residuals of energy and DO model were less than 10^{-6}, and the residuals of other solution variables concurrently were less than 10^{-4}.

$$div(\rho u_i \phi) = div(\Gamma grad\phi) + S \qquad (1)$$

where ρ is density (kg/m^3); u_i is the velocity in i direction; Γ is diffusion coefficient; S is source term; ϕ represents physical variables (*e.g.*, velocity, temperature and CO_2 concentration). More details about the equations and parameters can be found in the reference.[32]

Test for grid independence

Hexahedral grids were used to discretize the computational domain. Some locations with an obvious change in variables were locally refined, such as the regions near the inlet, outlet, heat source and walls. Figure 3 shows the mesh in the computational domain of four ventilation methods. The refined first layer of the grid was at most 15 mm. The growth rate was kept in the range of 1.0 – 1.4. The width of the maximum cell was less than 200 mm, guaranteeing that the aspect ratio of the cell was no more than 15. In this study, all the elemental qualities of the grids were higher than 0.9. The parameters of the grid of the different models for four ventilation methods are listed in Table 3.
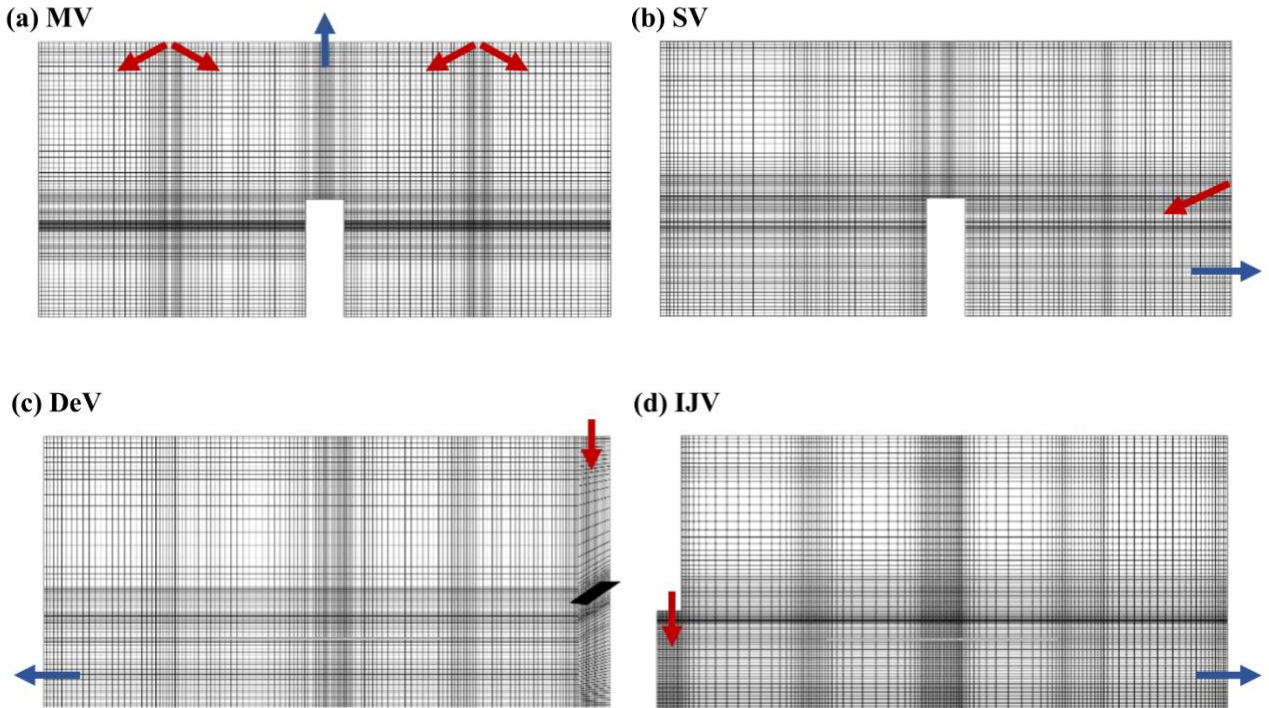

Figure 3. Sections of mesh model passing through the centre of supply air inlet, (a) MV, (b) SV, (c) DeV, (d) IJV.

The size of grids could greatly influence the accuracy of simulation results when using CFD method. To test the grids' independence, the mesh for each ventilation method was checked by three division schemes. The profiles of the air parameters along the vertical centreline of the room were

compared in Figure 4. Considering the computational accuracy and cost, the ultimate numbers of elements were specified as 1.639 million, 1.568 million, 1.531 million and 1.551 million for MV, SV, DeV and IJV, respectively.

Table 3. Grid information on ventilation methods.

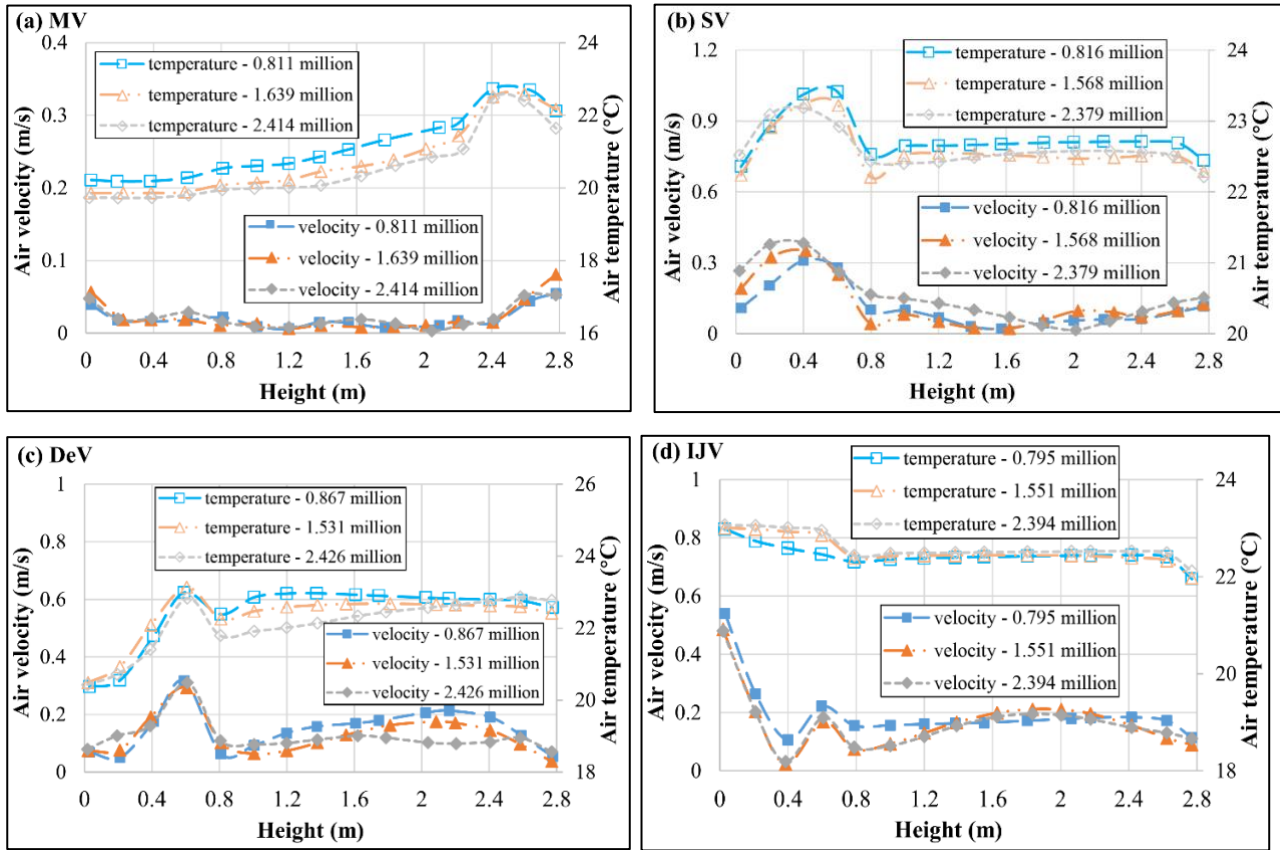| Ventilation method	Number of elements	Growth ratio	Maximum aspect ratio	Width of maximum cell	Non-dimensional distances of walls (y+)
MV	1,639,332	1.0 – 1.35	7.9	0.08 m	11.95
SV	1,567,708	1.0 – 1.3	11.2	0.11 m	14.26
DeV	1,530,738	1.0 – 1.3	13.6	0.13 m	13.14
IJV	1,551,099	1.0 – 1.3	12.0	0.12 m	21.28

Figure 4. Comparisons of simulated air parameters for three types of grid number, (a) MV, (b) SV, (c) DeV, (d) IJV.

Validation for numerical simulations

The indoor airflow field and contaminant distribution were validated using experimental data. With the same setup as the experiments (Case 3, Case 6 and Case 9), the simulated air velocity and temperature were compared with the collected data of MV, SV and DeV, respectively. Because of a limited paper length, only the results of Sampling Line L1 are presented in Figure 5. The Root Mean Square Error (RMSE) of air temperatures and velocities along the ten sampling lines between CFD simulations and measurements were 1.309 and 0.075 for MV, 0.527 and 0.072 for SV, 0.699 and 0.047 for DeV, respectively. Overall, the simulated air temperature and velocity aligned well with the measurements, indicating that the CFD simulations were reliable for simulating the air flow under these three ventilation methods for winter heating.
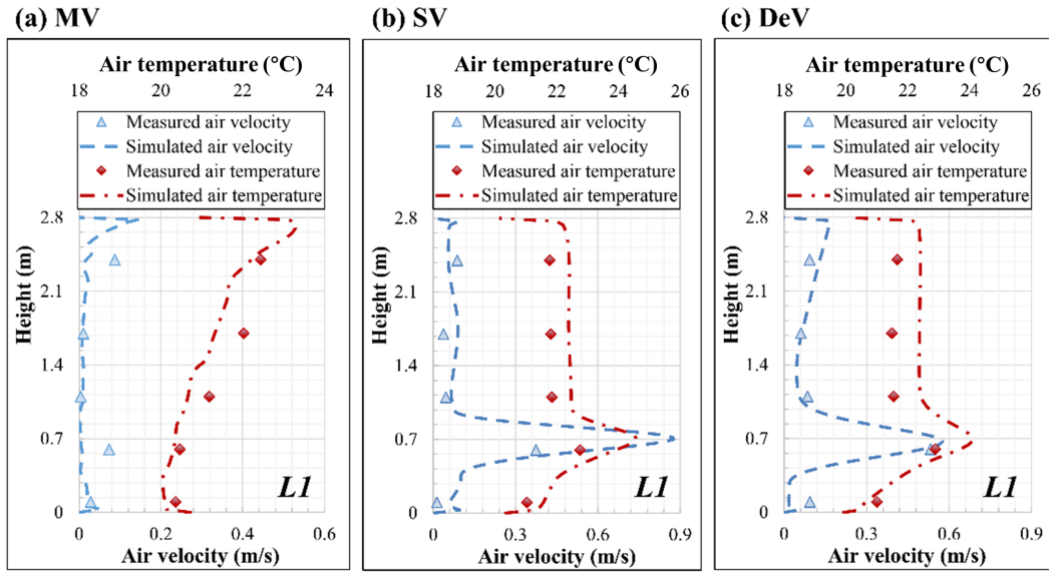

Figure 5. Comparisons of experimental and simulated air parameters along Sampling Line L1, (a) MV, (b) SV, (c) DeV.

For the validation of the airflow field in the room heated by IJV, the measured data were acquired from the experiments of Ye[22]. Measurements were conducted in a chamber which had the dimensions of 3.6 m (X) × 3.0 m (Y) × 2.5 m (Z). The airflow of IJV was supplied into the room through a nozzle at 0.17 m above the floor. The supply air temperature and velocity were maintained at 35.6°C and 1.2 m/s, respectively. At the centre of the ceiling, a rectangle exhaust air outlet (0.2 m × 0.3 m) was used to extract indoor air. When the monitored parameter in the room was steady, the air velocity and temperature data were collected through hot wire anemometers and K-type thermocouples arranged on four movable measuring poles in the room. Figure 6 shows the layout of the climate chamber and the sampling lines, and the comparison between predicted air parameters and measured data. The

RMSE of normalized air temperatures and velocities along the four sampling lines between CFD simulations and measurements was 0.068 and 0.026, respectively. The simulated and experimental air parameter values were in good agreement. Thus, the CFD simulations can be reliably applied to predict the air flow of IJV in winter.
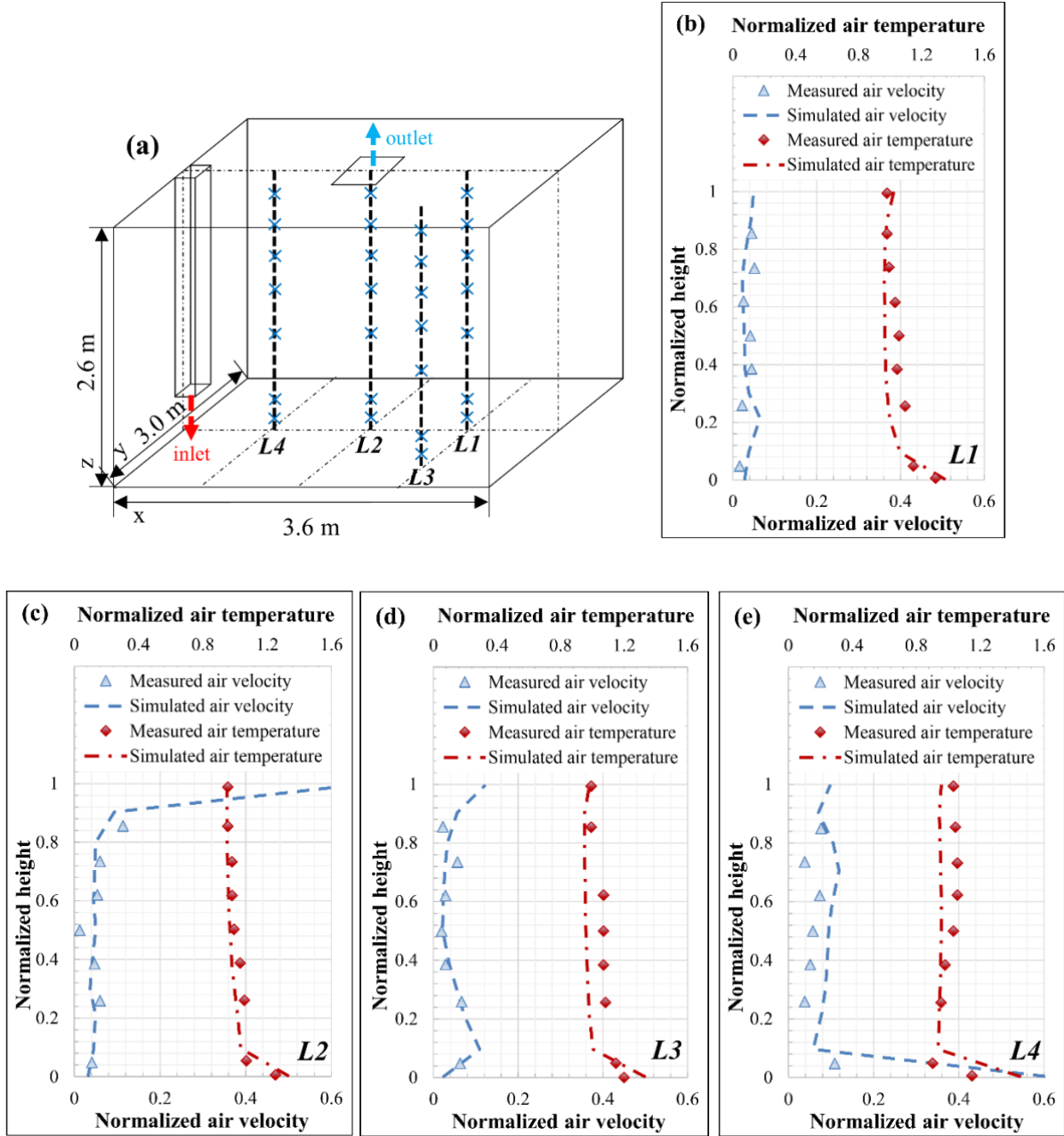

Figure 6. (a) Geometry of test chamber,[22] Comparisons of experimental and simulated air parameters along (b) Sampling Line L1, (c) Sampling Line L2, (d) Sampling Line L3, (e) Sampling Line L4.
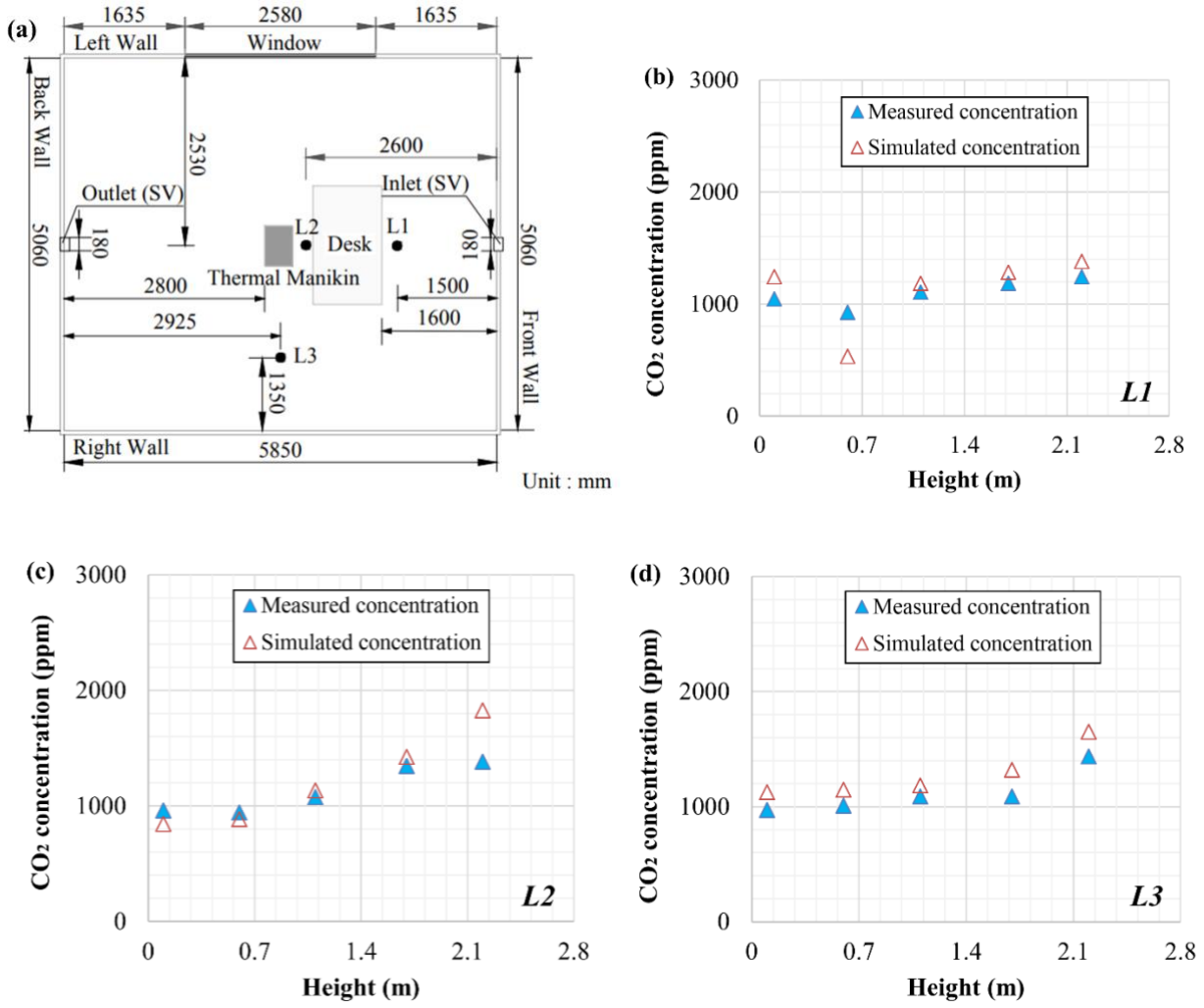
Figure 7. (a) Geometry of test chamber, Comparisons of experimental and simulated CO_2 concentration along (b) Sampling Line L1, (c) Sampling Line L2, (d) Sampling Line L3.

For the validation of the pollutant transport model, an experiment was conducted in the full-scale test chamber. The dimensions of the chamber were the same as that described in Section 'Description of the geometry'. In the chamber, all the temperatures of walls and windows were recorded by WZY-1 recorders, which were set as the boundary conditions. As shown in Figure 7(a), the supply air inlet (0.18 m × 0.18 m) was located at the side wall, and the exhaust outlet (0.18 m × 0.18 m) was located at the opposite wall. During the experiment, the supply air velocity was set at 2.1 m/s, and the supply air temperature was maintained at 25.0°C. A thermal manikin was placed in the centre of the chamber. The CO_2 was introduced via a small hole with a diameter of 0.008 m at the height of 1.1 m of the manikin, with a horizontal initial velocity of 1.0 m/s. The CO_2 concentrations were collected by three sampling lines (L1 – L3) in the chamber. By the pSENSE II instruments,

stable CO_2 concentrations along these sampling lines were obtained. The measurement error of pSENSE II was ± 30 ppm within the range of 0 – 9,999 ppm. The experimental data were used to validate the species transport model. A comparison of experimental and simulated CO_2 concentrations along the three sampling lines is shown in Figure 7(b) – (d). The average relative error of the CO_2 concentrations for all measurement points was 6.8%. The predicted concentrations were in good agreement with the experimental values. Thus, the species transport model can reasonably predict CO_2 dispersion.

Evaluation indexes

This study used indoor air temperature and velocity distributions to characterize the airflow fields. Overall thermal comfort was evaluated based on the predicted mean vote (PMV). Draught rate (DR) and vertical air temperature difference (ΔT) were indicators used to evaluate local thermal comfort. The air diffusion performance index (ADPI) was employed to evaluate the uniformity of air distribution. The energy utilization coefficient (EUC) was employed to evaluate the energy utilization effectiveness of supply air.[33] In addition, the CO_2 concentrations at the breathing zone were predicted, and the local mean age of air (LMAA) at the breathing zone was calculated by a user-defined scalar (UDS) in CFD simulation. The contaminant removal efficiency (CRE) and air change efficiency (ACE) at the breathing zone were employed to evaluate inhaled air quality. The air parameters in the occupied zone were adopted to calculate the thermal comfort and energy-saving characteristics indexes. The simulated results at the breathing zone were adopted to calculate the inhaled air quality indexes. The occupied zone was defined as the space between the floor and the height of 1.8 m from the floor with 0.3 m away from the walls, and the breathing zone was defined as the plane at a height of 1.1 m above the floor.[13]

The calculation of PMV was according to ISO 7730:2005.[34] In winter, the typical metabolic rate for office work and clothing insulation values are 1.2 met and 1.0 clo, respectively.[34] The mean radiant temperature was assumed to be equal to the indoor air temperature.[35, 36] For the relative humidity, the measured results in experiments were used (see Table 1).

DR was used to quantify the local thermal comfort, representing the percentage of unwanted local cooling due to draught, which was calculated as given by Equations (2) and (3).[13, 37]

$$T_u = \frac{V_{sd}}{V_i} \times 100\%$$

(2)

$$DR = (34 - T_i)(3.14 + 0.37v_i T_u)(v_i - 0.05)^{0.62}$$

(3)

Where T_u is turbulence intensity, %; V_i is average air velocity, m/s; T_i is air temperature, °C.

ΔT was an index to evaluate local thermal discomfort caused by a large air temperature difference between the head and ankle levels as defined by Equations (4) and (5). This study defines the ankle level as 0.1 m above the floor. Furthermore, for seated and standing occupants, the head levels are defined as 1.1 and 1.7 m above the floor, respectively.[13]

$$\Delta T_1 = T_{1.1} - T_{0.1} \tag{4}$$
$$\Delta T_2 = T_{1.7} - T_{0.1} \tag{5}$$

Where ΔT_1 and ΔT_2 are the ΔT for seated and standing occupants, respectively, °C; $T_{0.1}$, $T_{1.1}$ and $T_{1.7}$ are the air temperatures at the height of 0.1, 1.1 and 1.7 m above the floor, respectively, °C.

The effective draught temperature (EDT), °C, as determined by Equation (6), was used to define ADPI as given by Equation (7), which is the ratio of comfort points (meeting the requirement of EDT, with air velocity no more than 0.35 m/s) to the total measuring points in a space, which can be used to evaluate the uniformity of airflow and thermal comfort.[38]

$$EDT = T_i - T_r - 9.1(v_i - 0.15) \tag{6}$$
$$ADPI = \frac{N_{-2.2<EDT<2.0}}{N_{total}} \times 100\% \tag{7}$$

Where T_r is the average air temperature in the occupied zone, °C.

EUC as defined by Equation (8) was used to quantify the efficiency of energy utilization for supply air, which had been considered an effective index for evaluating ventilation methods.[15, 33]

$$EUC = \frac{T_s - T_e}{T_s - T_r} \tag{8}$$

Where T_s and T_e are the supply air temperature and the exhaust air temperature, respectively, °C.

CRE can reflect the contaminant removal ability of the ventilation method.[39] The CRE at the breathing zone was calculated as given by Equation (9).

$$CRE = \frac{C_e - C_s}{C_{1.1} - C_s} \tag{9}$$

Where C_e, C_s and $C_{1.1}$ are CO_2 concentrations at the exhaust outlet, supply air inlet and breathing zone, respectively. In this study, C_s was set as 460 ppm, the measured CO_2 concentration at the supply air inlet of the test chamber in Chongqing.

ACE was used to quantify how quickly the air at the breathing zone was replaced.[39] It reflected

the fresh of the air in the target zone, which can be calculated as given by Equation (10).

$$ACE = \frac{\tau}{\overline{\tau_{1.1}}} \tag{10}$$

Where τ is the nominal time constant, $\tau = V/q$, V is the room volume, m^3, and q is the supply airflow rate, m^3/s; $\overline{\tau_{1.1}}$ is the LMAA at the breathing zone, s. The LMAA at the supply air inlet was set as 0.

In this study, each evaluation index and its limit values are summarized in Table 4.

Table 4. Evaluation index and limit value.

Aspect	Evaluation index	Category and limit value[28, 34, 39]
Thermal comfort	Predicted Mean Vote (PMV)	Category A (-0.2 < PMV < +0.2) Category B (-0.5 < PMV < +0.5) Category C (-0.7 < PMV < +0.7)
	Draught Rate (DR)	Category A (DR < 10%) Category B (10% ≤ DR < 20%) Category C (20% ≤ DR < 30%)
	Vertical air temperature difference (△T)	Category A (△T < 2°C) Category B (2°C ≤ △T < 3°C) Category C (3°C ≤ △T < 4°C)
Energy-saving	Air Diffusion Performance Index (ADPI)	Minimum limit, 80%
	Energy Utilization Coefficient (EUC)	The higher, the better
Inhaled air quality	Contaminant Removal Efficiency (CRE)	The higher, the better
	Air Change Efficiency (ACE)	The higher, the better

Results and discussion

Airflow field

Figures 8 and 9 show the typical indoor air temperature and velocity distributions for the four ventilation methods. Significant differences were found in the room heated by different ventilation methods. Concurrently, due to the opposite direction of thermal buoyancy, the indoor airflow distribution characteristics showed differences from the cooling mode.[13, 23] The warm supply airflow of MV attached to the ceiling and the airflow entering the occupied zone was less in heating mode.

16

As a result, an evident phenomenon of air temperature stratification can be found under MV. The air temperature and velocity in the occupied zone were lower concurrently. The higher average air temperatures of the occupied zone were found in the room served by SV and DeV, both above 21°C. Although the direction of the supply air jets of SV was impacted due to positive thermal buoyancy, they can still enter the occupied zone due to effective airflow pattern.[13]
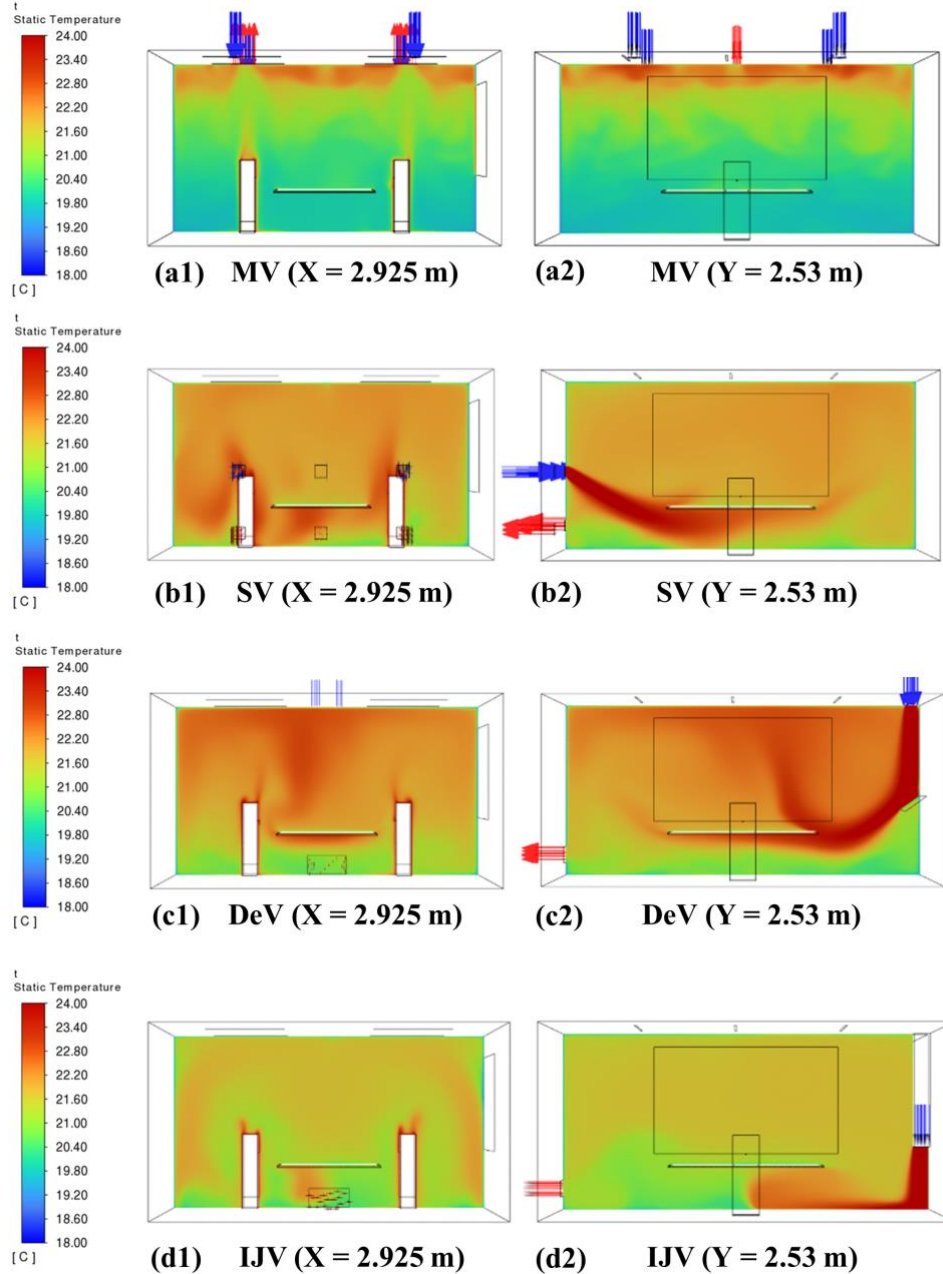

Figure 8. Contours of typical air temperature distributions in the middle sections of the room, (a) MV – Case 3, (b) SV – Case 6, (c) DeV – Case 9, (d) IJV – Case 12.

For DeV, the supplied air flow was downward along the wall due to Coanda effect and was

compelled to be transported into the occupied zone through a deflector. Compared with SV, the airflow of DeV rose earlier, and the air temperature and velocity in the lower zone of the room were slightly lower because of the long distance between the supply inlet and the occupants.[40] After the collision between the supply airflow of IJV and the floor, the airflow extended along the floor and formed a warm air lake. In the room, the air temperature on the left side was significantly lower than that on the right side, meaning that in winter, a non-uniform environment was created under IJV.
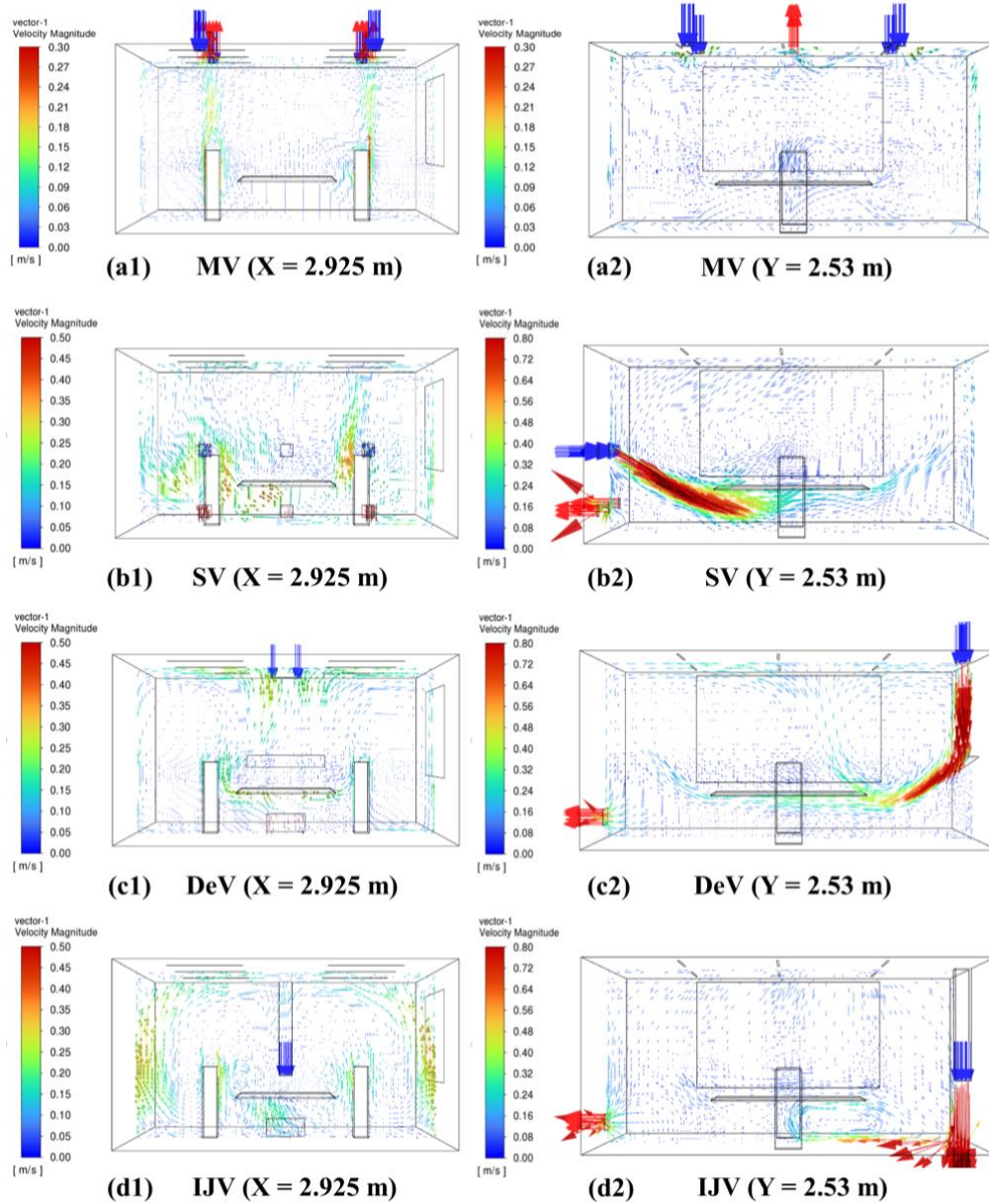

Figure 9. Typical air velocity vector distributions in the middle sections of the room, (a) MV – Case 3, (b) SV – Case 6, (c) DeV – Case 9, (d) IJV – Case 12.
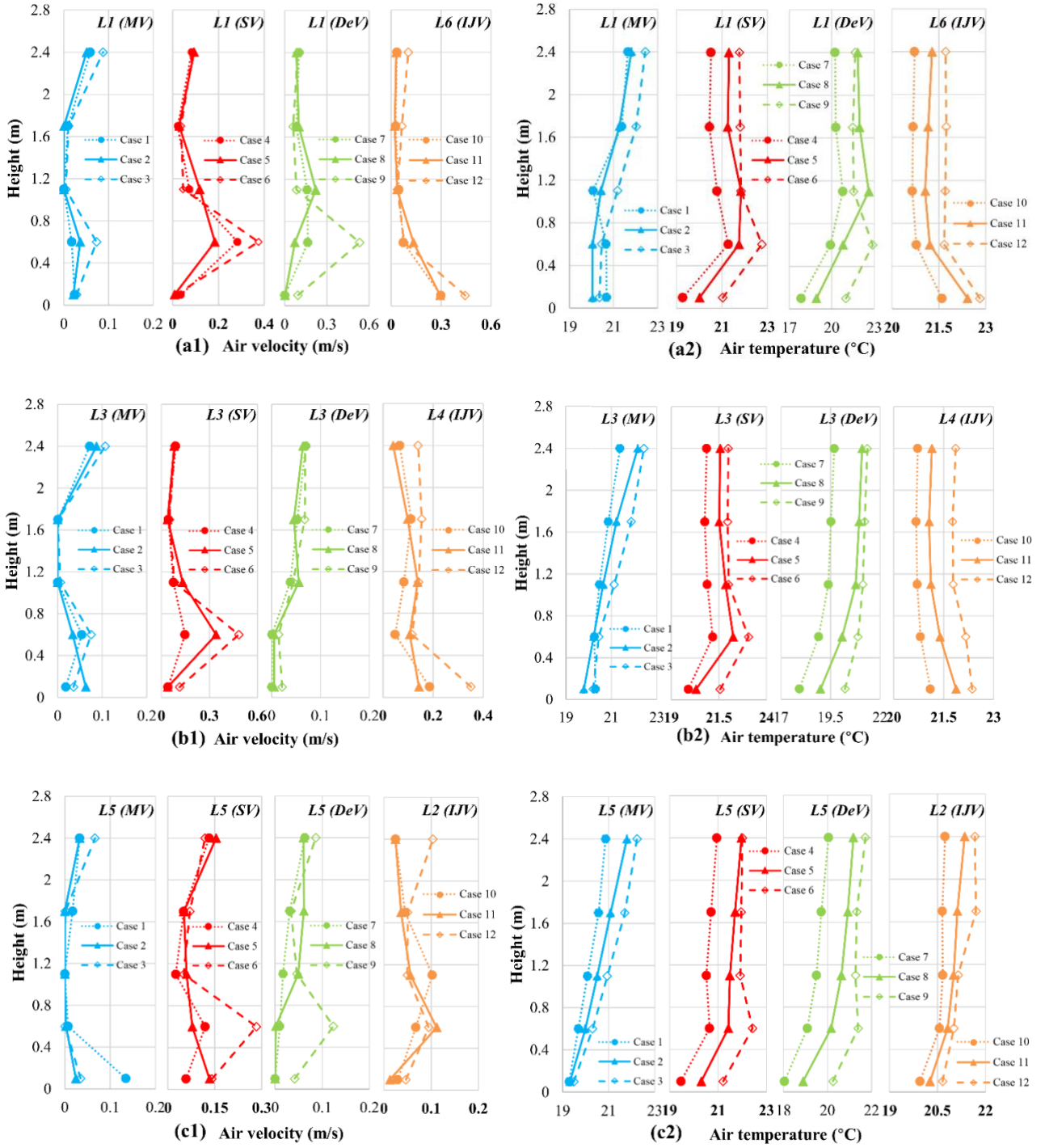
Figure 10. Air velocity and temperature profiles for Cases 1 – 12. (a) In the near field of supply air jet, (b) Near thermal manikin, (c) In the far field of supply air jet.

Figure 10 shows air temperature and velocity profiles along typical sampling lines for the four ventilation methods at three different heating supply air parameters. Three sampling lines were distributed in the near field of the supply air jet, near the thermal manikin and in the far field of the supply air jet, respectively. For MV, indoor thermal stratification was evident. The air temperature

was increased almost linearly as the height, with a maximum vertical air temperature gradient of 0.98°C/m in Case 3. This showed that a large amount of warm air was accumulated in the upper zone of MV heated room.[23] In the occupied zone, the air velocity was generally lower than 0.08 m/s under MV, indicating that the warm supply air was difficult to flow down. The locations with high air temperature and/or velocity can reflect the trajectory of the supply air jet. For SV, the higher values along three sampling lines were at the height of 0.6 m. This indicated that the supplied air of SV penetrated the entire occupied zone effectively. For DeV, the highest air temperature and velocity were found at the height of 1.1 m when the ACH was 3.88 (Cases 7 and 8). When the ACH was increased to 5.98 (Case 9), the highest values occurred at a lower height of 0.6 m. With the effect of a downward deflector, the warm supply air jet entered the lower occupied zone at a short distance from the wall. In the room served by IJV, the highest air temperature and velocity along L6 and L4 were at the height of 0.1 m, while those along L2 were observed in the upper zone of the room. This indicated that the warm air was difficult to penetrate the rear-occupied zone due to the positive thermal buoyancy and the decay of the supply air jet.

Thermal comfort

Predicted mean vote (PMV)

Figure 11 shows the distribution of PMVs in the occupied zone for the four ventilation methods. The air parameters from 40 measurement points along Sampling Lines L1 – L10 in the occupied zone were used to calculate PMVs. For the cases of MV, the average PMVs were in the range of -0.7 – 0.7, which complied with Category C of ISO 7730:2005.[34] For SV, DeV and IJV, the average PMVs were in the range of -0.5 – 0.5, which were at least in compliance with Category B of ISO 7730:2005. Although the average PMVs complied with the comfortable requirements, the room heated by MV was colder in winter. Under the influence of positive thermal buoyancy, the supply airflow of MV was detained in the upper zone of the room, and less warm air was supplied to the occupied zone. The average PMVs of Case 5 (SV), Case 6 (SV) and Case 9 (DeV) were -0.2, -0.1 and -0.1, respectively, conforming to Category A of ISO 7730:2005. The improvement in thermal comfort was attributed to the combined effect of air temperature and velocity.[33] Under the same air supply conditions, the supply airflows of SV and DeV can provide more heat to the occupied zone, which was beneficial to improve PMV.
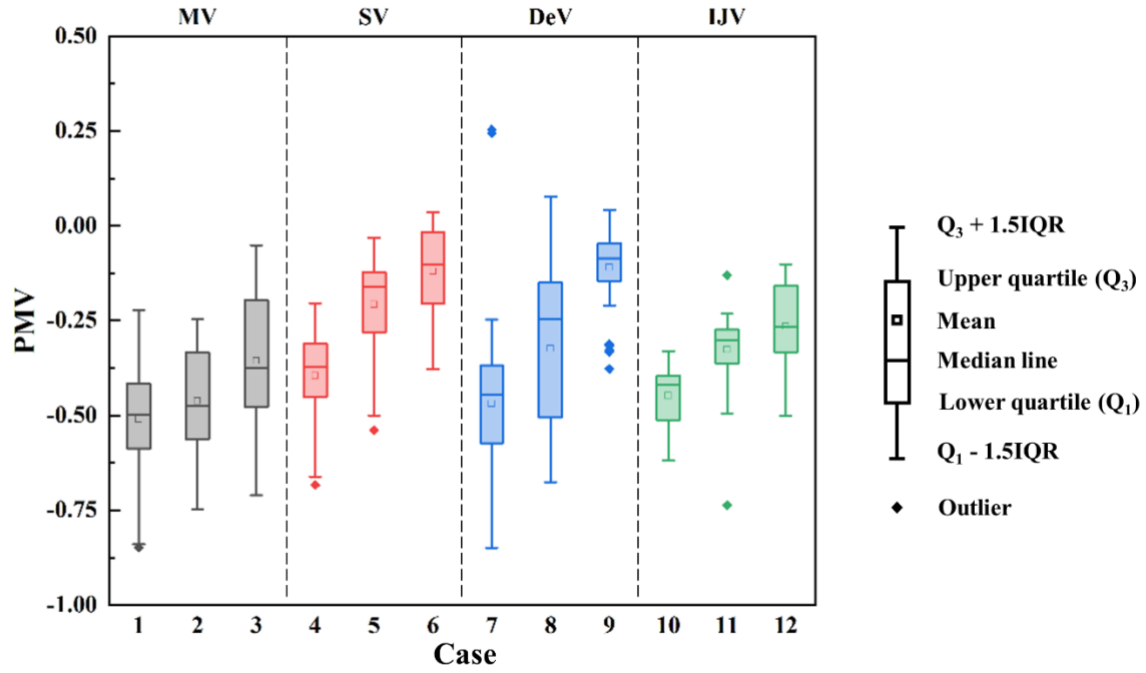
Figure 11. Comparison of PMVs for Cases 1 – 12.

Draught rate (DR)

The ankle and head are sensitive to draught.[34] Therefore, in this study, DRs were calculated by the air parameters at 0.1 and 1.1 m above the floor, as shown in Figure 12. The low DRs were found in the cases of MV and DeV. The average DRs at the ankle and head levels were lower than 10%, which complied with Category A of ISO 7730:2005. For MV, the low DRs were attributed to the low air velocity in the occupied zone in winter. For DeV, the air temperature in the occupied zone was relatively high whilst the velocity in the lower zone was relatively low, thereby resulting in the average DRs of below 5%. For SV, although the air velocity in the occupied zone was relatively higher, the average DRs of Cases 4 – 6 were all lower than 20%, which were at least in compliance with Category B of ISO 7730:2005. For heating mode, the higher air temperature in the occupied zone under SV can reduce discomfort caused by draught.[13] The DRs at the ankle level in the room heated by IJV was significantly higher than that of the other three ventilation methods. With the same supply air parameters, the average DRs at the ankle level for the cases of IJV were the maximum, and the DR value reached 35% at a high ACH. Additionally, the range of DR under IJV was wider, indicating the air temperature and velocity distributions at 0.1 m height were non-uniform. At 0.1 m above the floor, the larger DR values appeared near the supply inlet. In contrast, the DR values far away from the supply inlet were significantly low, which was attributed to the flow characteristics of IJV. The DR values of IJV in summer can be higher due to lower supply air temperature, and the

21

horizontal temperature distribution in summer can be more uniform due to the opposite direction of thermal buoyancy.[41]
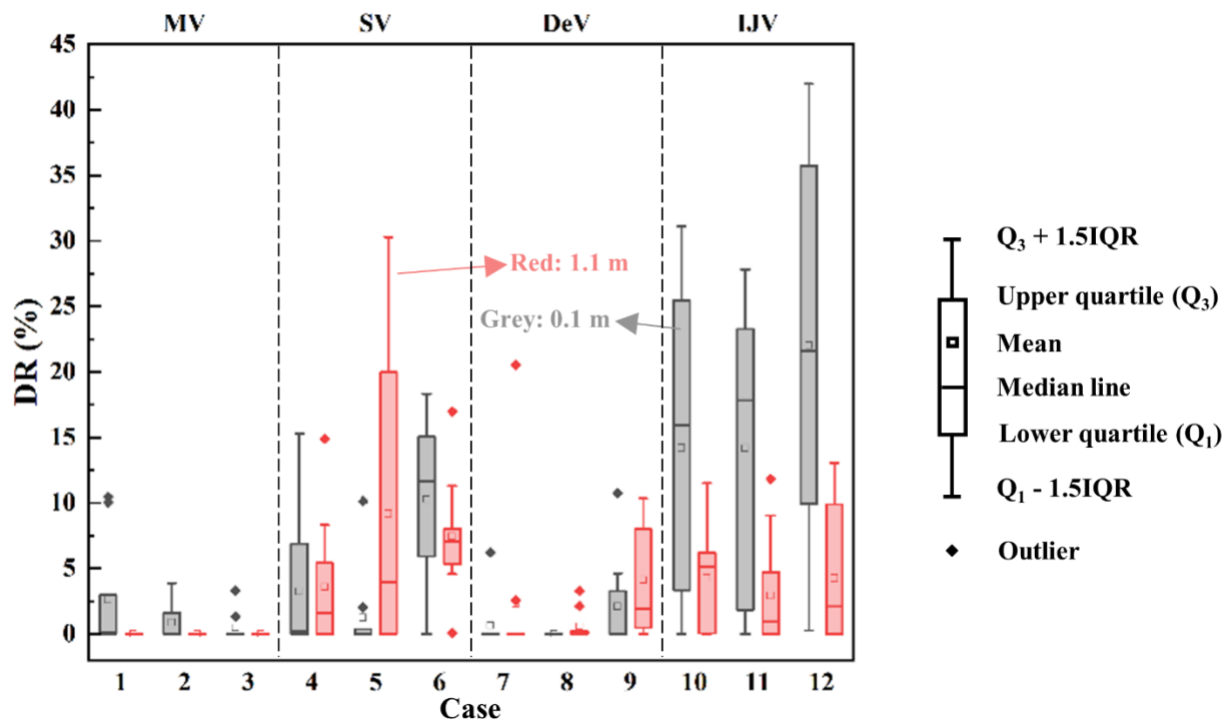

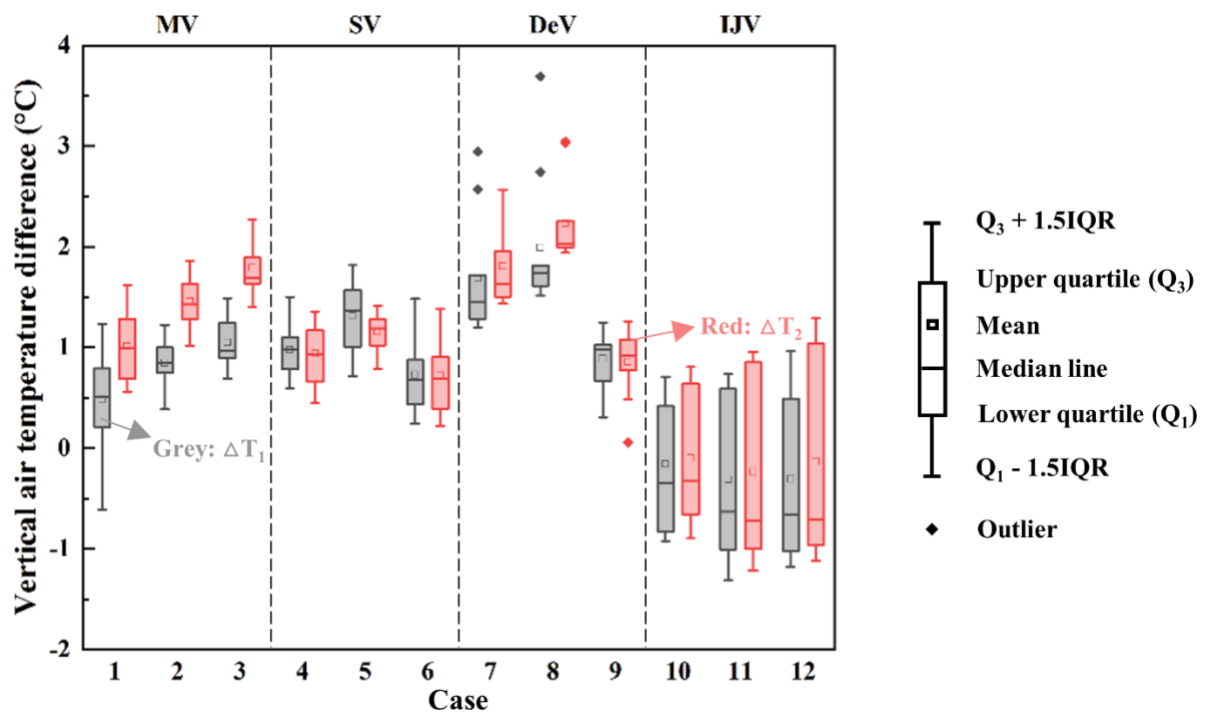**Figure 12.** Comparison of DRs at the ankle and head levels for Cases 1 – 12.

Figure 13. Comparison of $\triangle$Ts for seated occupants ($\triangle T_1$) and standing occupants ($\triangle T_2$).

Vertical air temperature difference ($\triangle$T)

Figure 13 shows the $\triangle$T values of Cases 1 – 12 for seated occupants ($\triangle T_1$) and standing occupants ($\triangle T_2$). For all cases, the average values of $\triangle T_1$ and $\triangle T_2$ were lower than 3°C, which complies with Category B as specified in ISO 7730:2005. This indicated that the four ventilation methods might not cause discomfort in warm head and cold feet usually. For the cases of SV, the values of $\triangle T_1$ and $\triangle T_2$ were less than 2°C, conforming to Category A given in ISO 7730:2005. For the cases of IJV, the absolute values of $\triangle T_1$ and $\triangle T_2$ were less than 1°C, conforming to Category A of ISO 7730:2005. The average values of $\triangle T_1$ and $\triangle T_2$ were negative, indicating that the air temperature at local zones on the floor was warm. Additionally, the range of $\triangle T$ under IJV was wider, which was attributed to the non-uniform air temperature distributions at 0.1 m above the floor.

Air diffusion performance index (ADPI)
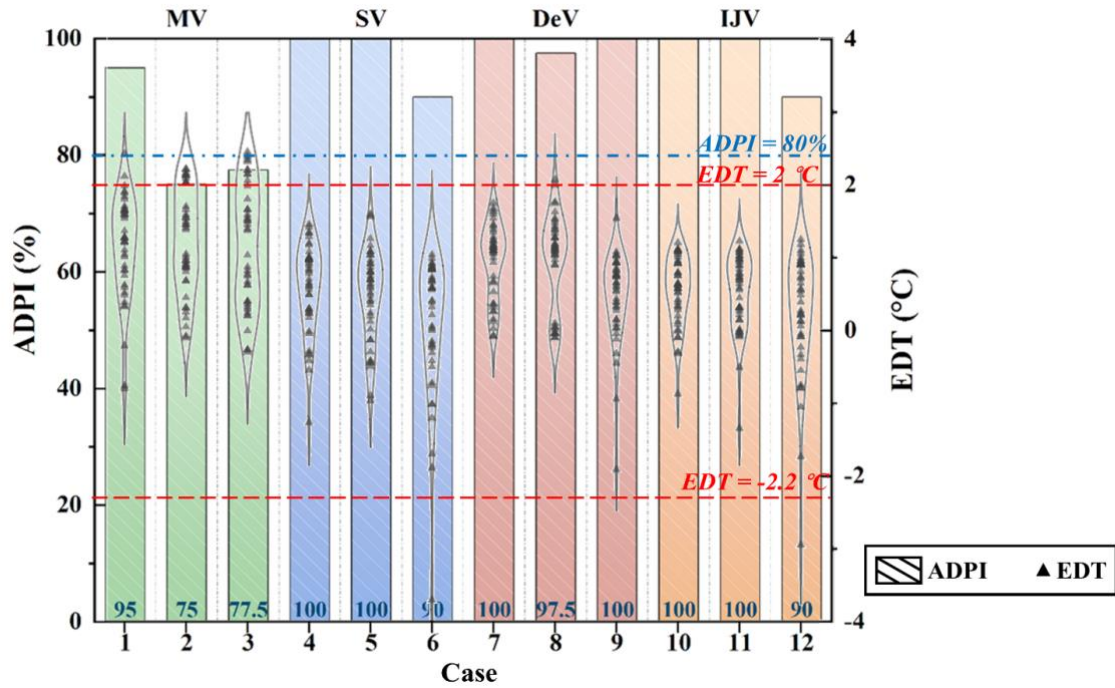
Figure 14. Comparison of EDTs and ADPIs for Cases 1 – 12.

On Sampling Lines L1 – L10, 40 measurement points in the occupied zone were used to calculate the EDTs and ADPIs for each case, as shown in Figure 14. A higher value of ADPI indicates more uniform thermal environment. ANSI/ASHRAE 113-2022 stipulates that the limit value of ADPI meeting thermal comfort is 80%.[28] The ADPIs of the cases of MV were 95%, 75% and 77.5%, respectively. For Cases 2 and 3, as the supply air temperature was increased from 24°C to 26°C, the supply airflows of MV were more seriously influenced by positive thermal buoyancy, which caused

the EDTs of some measuring points in the upper occupied zone of the room to be higher than 2°C. Although the air diffusion performance was improved and the ADPI value was increased by 2.5% when the ventilation rate was increased from 3.88 to 5.98 ACH, it still cannot meet the specified requirement of ANSI/ASHRAE 113-2022. The low ADPI values showed that the thermal environments of MV were non-uniformity, which differed from that in summer.[42] Additionally, it was seen that for the cases of SV, DeV and IJV (Cases 4 – 12), the ADPIs were at least 90%. Therefore, SV, DeV and IJV can comply fully with the stipulation of ADPI in heating mode.

Under three different supply air conditions, overall and local thermal comfort of four ventilation methods were comprehensively compared through four different thermal comfort evaluation indexes. The results showed that SV and DeV exhibited better performances for thermal comfort. The PMVs, DRs and △Ts of the cases of SV and DeV were at least in compliance with Category B of ISO 7730:2005, and the ADPIs were in full compliance with the stipulation of ANSI/ASHRAE 113-2022.

Energy-saving characteristics

Based on the supply air temperature, the exhaust air temperature and the average air temperature in the occupied zone, EUCs were calculated by Equation (8). Figure 15 shows the EUCs for Cases 1 – 12. The higher the EUC is, the more effectively the supply of air is used to heat the occupied zone. When EUC is higher than unity, the ventilation methods would be considered energy-efficient.[33] Under the three supply air parameters, the EUCs of the cases of MV were significantly lower, with the maximum EUC of only 0.6. Influenced by positive thermal buoyancy, plenty of warm supply airflow of MV was accumulated in the upper zone, resulting in a lower air temperature in the occupied zone and a higher exhaust air temperature. The exhaust air temperatures of MV were all above 21.8°C, which was higher than the corresponding average air temperature of the occupied zone (see Table 1). For SV, DeV and IJV, the exhaust air temperatures were all lower than the corresponding average air temperature of the occupied zone. Thus, the supply airflows of SV, DeV and IJV could provide heat energy for the occupied zone more effectively. All the cases of SV, DeV and IJV had EUC values higher than unity, which indicated their excellent energy-saving characteristics. For advanced ventilation methods, Liu and Lin[43] found that EUC value of SV was around 1.31 for cooling mode. The results of Qin and Lu[33] showed that EUC values of IJV in cooling mode were in the range of 1.14 −1.31 under different layouts of exhaust outlet. The EUC values in heating mode were slightly lower than that in the cooling mode, which may be due to the difference of indoor air temperature distributions in winter caused by positive thermal buoyancy.[33]
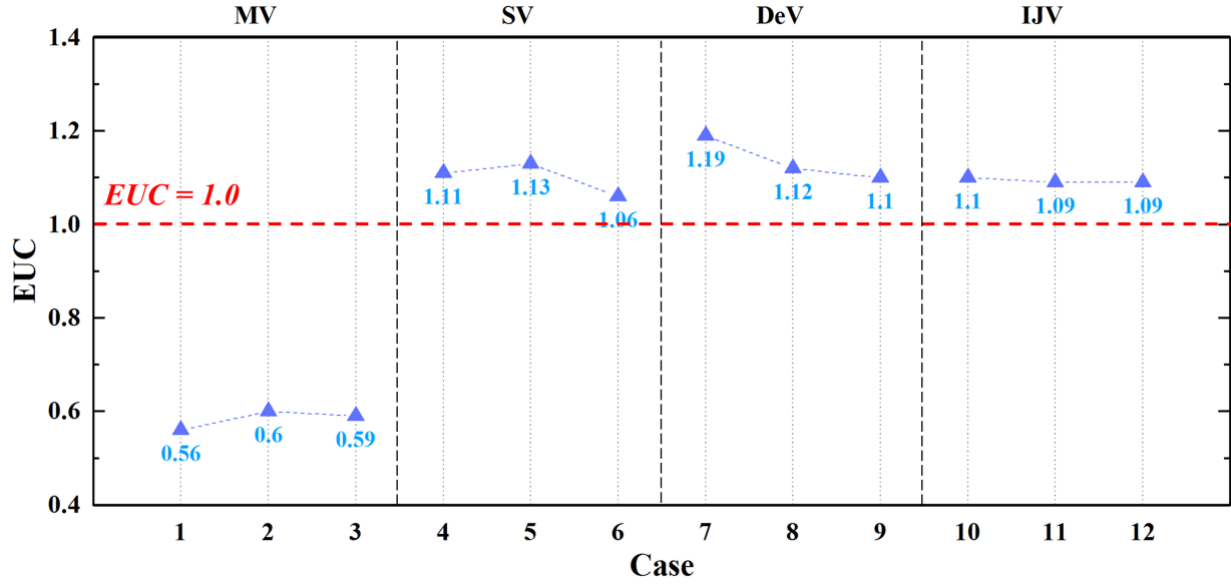
Figure 15. Comparison of EUCs for Cases 1 – 12.

Inhaled air quality

Air change efficiency (ACE) at the breathing zone

Figure 16 shows the LMAAs and ACEs at the breathing zone for Cases 1 – 12. The lower the LMAA is, the fresher the inhaled air at the breathing zone is. The higher the ACE is, the stronger the ability of the ventilation method to exchange the air at the breathing zone.[39]
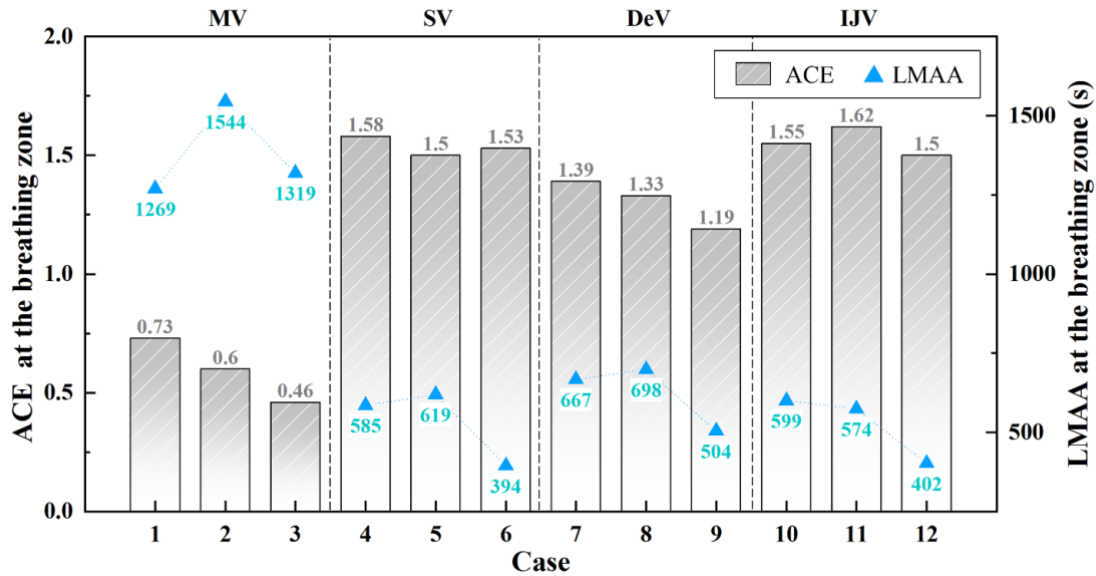
Figure 16. Comparison of LMAAs and ACEs at the breathing zone for Cases 1 – 12.

As only a tiny amount of supply air entered the occupied zone, the LMAAs were significantly

higher in the room heated by MV. Under the same supply air parameters, the LMAAs under MV were around 2.5 times that of SV and IJV. This indicated that the supply airflow of MV took more time to ventilate the breathing zone. As a result, the cases of MV had low ACEs, with a maximum ACE of only 0.73. Similar LMAAs and ACEs were found in the cases of SV and IJV. The ACEs of SV and IJV were both higher than 1.5. The LMAAs and ACEs of the cases of DeV were slightly lower than that of SV and IJV, but significantly better than that of MV. Compared with MV, the usage of the deflector under DeV can effectively guide the supply of airflow to the breathing zone. Advanced ventilation methods provided higher ACEs both in summer and winter compared with MV.[8] Additionally, the ACEs in cooling mode may be higher than the heating mode, as in winter, more air would leave the occupied zone and enter the upper zone of the room under the influence of positive thermal buoyancy.[17, 33]

Contaminant removal efficiency (CRE) at the breathing zone

Figure 17 shows the average CO_2 concentrations and CREs at the breathing zone for Cases 1 – 12. The average CO_2 concentration was applied to reflect the cleanliness of the air. The CRE reflected the relative relationship of CO_2 concentration between the breathing zone and the exhaust outlet.[44]
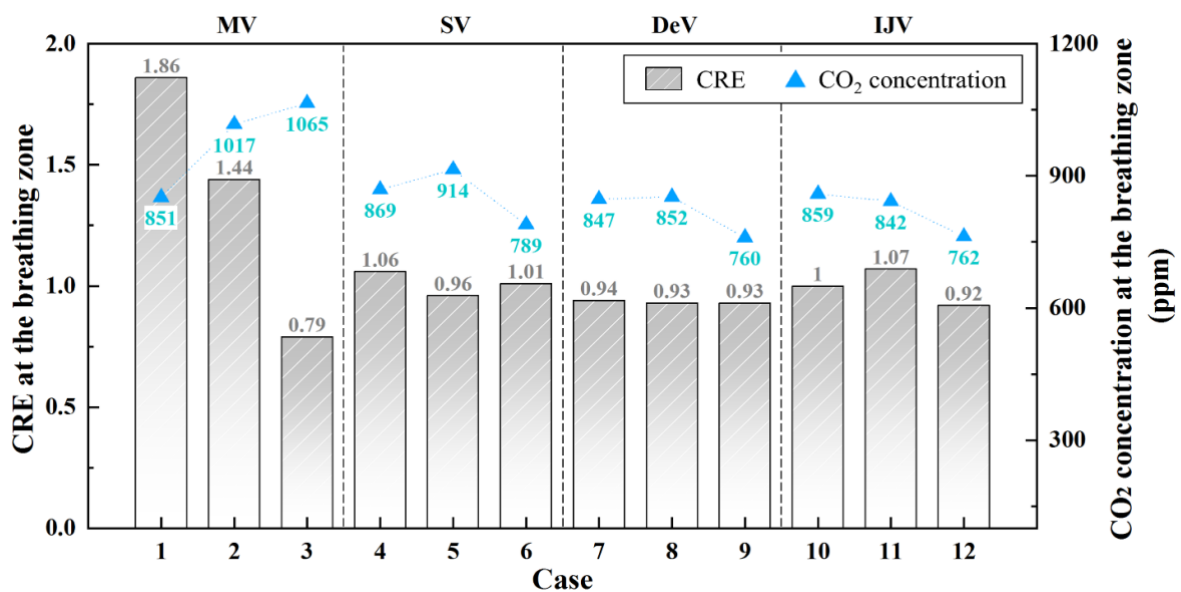
Figure 17. Comparison of CO_2 concentrations and CREs at the breathing zone for Cases 1 – 12.

Although the CO_2 concentrations under MV were high, the cases had relatively high CREs, especially at the low ACH. This might be due to the following reasons. Firstly, when the ACH was low, the air temperature at the lower zone of the room was lower, and the thermal plume of occupants was more vigorous. Under the extract effect of the thermal plume, the CO_2 can be carried up to the

upper space.[45, 46, 47] Secondly, at the low background air temperature, the exhaled CO_2 with a high temperature more easily rose due to thermal buoyancy.[45] Finally, the exhaust air outlets of MV were located directly above occupants. The CO_2 was just allowed to be carried by the thermal plumes and then exhausted favourably.[32] The influence of exhaust locations under MV on inhaled air quality is further discussed later. For SV, DeV and IJV, the average CO_2 concentrations at the breathing zone were in the range of 750 – 950 ppm, and the CREs were in the range of 0.9 – 1.1. Under the same supply air parameters, SV, DeV and IJV exhibited similar average CO_2 concentrations and CREs. At the breathing zone, the differences in the average CO_2 concentrations amongst them were less than 80 ppm, and the differences of the CREs were less than 0.15. In this study, the slightly lower CRE values of SV, DeV and IJV can be attributed to the exhaust air outlets located at the lower zone of the room. As the previous research recommended,[47] arranging the exhausts on the ceiling was beneficial to remove the pollutants.

Further discussion

Influence of exhaust location on inhaled air quality under MV

To explore the impact of the locations of exhaust air outlets in MV heated rooms on inhaled air quality, two other typical layouts of exhaust outlets were selected for further analysis.[44] For these two cases, the exhaust outlets were located on the ceiling and close to the side walls, and on the side walls and close to the floor, respectively, as shown in Figures 18(a2) and (a3). Figure 18(b) shows the indoor CO_2 concentration distributions of these cases with the same supply air parameters as Case 1 (the location of inlets and outlets was shown in Figure 18(a1)). The average CO_2 concentrations at the breathing zone for the three cases were 851, 1314 and 1397 ppm, respectively. The CO_2 concentration was significantly lower than the other two cases when the outlets were located directly above occupants. The exhaled CO_2 rose vertically and reached the air extraction location on the ceiling, which confirmed the positive effect of the thermal plumes and the location of outlets directly above the occupants on the removal of CO_2. The result was consistent with the conclusions of previous research.[45, 46, 47] For the heating mode, the thermal plume of heat source mainly carried indoor pollutants. Setting the exhaust air outlet near the heat source can be beneficial for extracting the pollutants directly.[46] Ahmed et al.[47] recommended that the exhaust air outlet can be arranged on the ceiling and closed to the heat source to achieve better indoor air quality. However, after changing the locations of the outlets, the CO_2 cannot be effectively removed after reaching the ceiling (see Figures 18(b2) and (b3)). It was obvious that the CO_2 was detained in the upper zone of the room.

The CRE at the breathing zone was decreased from 1.86 to 0.93 and 0.92, respectively, as shown in Table 5. This indicated that the locations of outlets in the room heated by MV significantly impacted pollutant removal. However, the exhaust locations may not significantly change the ability of the ventilation method to supply fresh air to the breathing zone.[48] This was because the ACE was mainly affected by the condition and layout of the supply air inlet.

In actual situations, the exhaust air outlets might not be located directly above occupants. Nevertheless, the results suggested that this layout can be used indoors. Especially, more and more people are concerned with the possible health effects of inhaled air quality. This means an active measure for occupants to improve the inhaled air quality by adjusting their working locations.
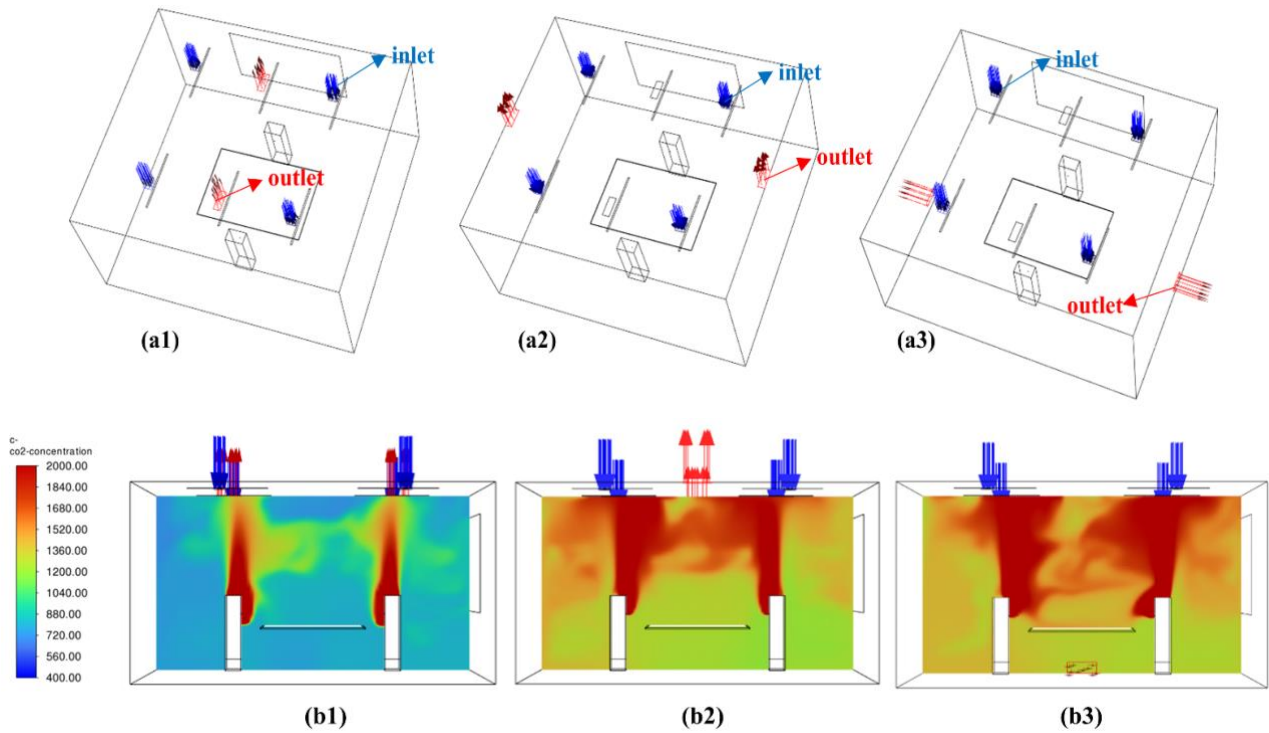
Figure 18. (a) Layout of the outlets under MV, (b) CO_2 concentration distributions (X = 2.925 m).

Table 5. Evaluation of inhaled air quality in MV heated room with different exhaust outlet locations.

Outlet locations	LMAA (s)	ACE	CO_2 concentration (ppm)	CRE
On the ceiling, above the occupants	1269	0.73	851	1.86
On the ceiling, close to the side walls	1495	0.65	1314	0.93
On the walls, close to the floor	1246	0.78	1397	0.92

Overall performance analysis

Table 6 provides a summary of the evaluation results of thermal comfort, inhaled air quality and energy-saving characteristics of Cases 1 – 12. The four ventilation methods produced different performances in different aspects. For example, although MV was free from draught, the EUCs and ACEs were the lowest amongst all ventilation methods. Therefore, it was not easy to specify directly the ventilation method with the best overall ventilation performance. To simultaneously consider the contribution of all evaluation indexes to the target, the entropy-weight method was used to assign the results objectively.[49]

Table 6. Summary of evaluation indexes for Cases 1 – 12.

Case	PMV	$DR_{0.1}$	$DR_{1.1}$	$\triangle T_1$	$\triangle T_2$	ADPI	EUC	ACE	LMAA	CRE	CO_2 concentration	D_i
1	-0.46	2.56	0	0.49	1.01	95	0.56	0.73	1269	1.86	851	0.30
2	-0.39	0.85	0	0.85	1.45	75	0.60	0.60	1544	1.44	1017	0.24
3	-0.29	0.46	0	1.05	1.79	77.5	0.59	0.46	1319	0.79	1065	0.26
4	-0.38	3.24	3.58	0.98	0.94	100	1.11	1.58	585	1.06	869	0.35
5	-0.19	1.25	9.16	1.31	1.16	100	1.13	1.50	619	0.96	914	0.32
6	-0.10	10.25	7.45	0.73	0.72	97.5	1.06	1.53	394	1.01	789	0.42
7	-0.45	0.62	2.31	1.69	1.81	100	1.19	1.39	667	0.94	847	0.25
8	-0.27	0	0.56	1.99	2.23	97.5	1.12	1.33	698	0.93	852	0.30
9	-0.08	2.09	4.11	0.89	0.86	100	1.10	1.19	504	0.93	760	0.47
10	-0.43	14.20	4.26	-0.16	-0.10	100	1.10	1.55	599	1.00	859	0.33
11	-0.31	14.16	2.92	-0.31	-0.24	100	1.09	1.62	574	1.07	842	0.38
12	-0.25	22.00	4.23	-0.31	-0.14	97.5	1.09	1.50	402	0.92	762	0.41

The entropy-weight method is widely used in the optimization and evaluation of ventilation methods.[49] The principle of the entropy-weight method is to determine the weight according to the variation of each index value. The smaller the entropy value, the greater the weight of this index. The entropy and weight were calculated as follows.

Step 1: Take the results as absolute values, as given by Equation (11). Distinguish between the benefit

indexes (*i.e.*, the higher, the better: ADPI, EUC, ACE and CRE) and cost-type indexes (*i.e.*, the lower, the better: PMV, $DR_{0.1}$, $DR_{1.1}$, $\triangle T_1$, $\triangle T_2$, LMAA, and the CO_2 concentration at the breathing zone).

$$y_{ij} = |x_{ij}| \tag{11}$$

Where x_{ij} is the value of the evaluation index x, y_{ij} is the absolute value of index x, i is the ith case, $1 \leq i \leq P$; j is the jth index, $1 \leq j \leq Q$; P represents the total number of cases and Q represents the total number of indexes.

Step 2: Normalize the results of indexes.

For benefit indexes, as normalized by Equation (12):

$$y_{ij}{}' = \frac{y_{ij} - min\{y_{ij}\}}{max\{y_{ij}\} - min\{y_{ij}\}} \tag{12}$$

For cost-type indexes, as normalized by Equation (13):

$$y_{ij}{}' = \frac{max\{y_{ij}\} - y_{ij}}{max\{y_{ij}\} - min\{y_{ij}\}} \tag{13}$$

Step 3: Calculate the probability of the ith case in each evaluation, as given by Equation (14).

$$Y_{ij} = \frac{y_{ij}{}'}{\sum_{i=1}^{n} y_{ij}{}'} \tag{14}$$

Step 4: Calculate the information entropy, e_j, as given by Equation (15).

$$e_j = \frac{1}{\ln n} \sum_{j=1}^{n} (Y_{ij} \ln Y_{ij}) \, , \left(0 \leq e_j \leq 1\right) \tag{15}$$

Step 5: Calculate the difference coefficient, g_i, as defined by Equation (16), and determine the weight, W_j, of each index as given by Equation (17).

$$g_i = 1 - e_j \tag{16}$$

$$W_j = \frac{g_i}{\sum_{j}^{m} g_i} \tag{17}$$

Step 6: Build the weighted arithmetic average model to calculate the overall score (D_i) of each case, as given by Equation (18).

$$D_i = \sum_{j=1}^{m} Y_{ij} W_j \tag{18}$$

The overall scores (D_i) of Cases 1 – 12 are listed in Table 6. The higher the D_i value, the better the

overall ventilation performance of the case would be. The upper limit of D_i is unity. The D_i value equals unity, meaning that all the evaluation indexes are optimal in this case. For Cases 1 – 12, the D_i values were 0.30, 0.24, 0.26, 0.35, 0.32, 0.42, 0.25, 0.30, 0.47, 0.33, 0.38 and 0.41, respectively. The maximum value of D_i was found in Case 9, indicating that DeV would produce more advantages for winter heating, followed by SV, IJV and then MV. The significant differences of D_i was found between the cases of DeV, which indicated that the supply air parameters greatly affected the heating performance of DeV. Previous studies also showed that DeV performed better at the higher supply air velocity.[40, 50] For IJV, the D_i values were slightly lower than SV, which was caused by the higher DR values at the ankle level. For MV, the maximum value of D_i was only 0.30, indicating that it was necessary to improve energy utilization efficiency and inhaled air quality in winter.

The occupied zone under MV was colder in winter, which was in good agreement with the results of previous research.[14, 16] According to the subjective survey results,[14] compared with MV, thermal comfort was enhanced by using stratum ventilation in winter. When the ACH was in the range of 6 – 15, DeV can achieve a better thermal comfort level and a better inhaled air quality with a lower supply airflow rate compared with MV in heating mode.[17] For IJV, limiting the supply air velocity within a range is necessary to avoid local thermal discomfort caused by draught.[51] Additionally, Su et al.[40] showed that the CO_2 concentrations in the zone near the infector under SV, DeV and IJV were similar when the ACH was 3.14. It was highlighted that DeV could be better if the ventilation rate was increased. A similar result was also concluded by Cheng et al.[50] In a recent study, Li et al.[18] demonstrated the better performances of DeV and SV on anti-airborne infection at a higher ACH. They found that DeV and SV can provide better inhaled air quality and higher particle removal efficiency than MV and IJV when the ACH was 7. The results derived from this study were consistent with those of the previous studies. The heating performances of these ventilation methods were compared with their cooling performances. Worse thermal comfort, energy utilization efficiency and air change efficiency were found in the room heated by MV compared with that in summer.[52, 53, 54] However, the contaminant removal efficiency of MV can be improved in winter under a particular layout of exhaust outlets in this study. For SV and IJV, due to the higher supply air temperature, local thermal comfort levels can be improved in winter.[13] In addition, the upward thermal buoyancy made part of warm supply air go up into the unoccupied zone rather than into the micro-environment around the occupants. This resulted in poor heating performances for advanced ventilation methods. The study found that the energy utilization efficiency and inhaled air quality under SV, DeV and IJV were slightly lower than that in summer.[17, 33, 55]

Conclusions

This study experimentally and numerically compared the heating performances of four ventilation methods (*i.e.*, MV, SV, DeV and IJV) in a typical two-person office in winter. Under different supply air parameters, the thermal environment, inhaled air quality and energy-saving characteristics of ventilation methods were compared comprehensively. The entropy-weight method was used for overall performance analysis. The findings derived from this study are summarized as follows.

(1) In winter, there were differences in indoor airflow characteristics and heating performances for different ventilation methods. The differences also existed between cooling and heating performances for the same ventilation method. For heating mode, advanced ventilation methods can better overcome the impact of thermal buoyancy compared with MV. Compared with cooling mode, the high supply air temperature in winter was beneficial for reducing draught risk, but the influence of thermal buoyancy may decline in energy utilization efficiency and inhaled air quality.

(2) Better thermal comfort was found in the rooms served by SV and DeV. The PMVs, DRs and △Ts for the cases of SV and DeV, which at least in compliance with Category B of ISO 7730:2005, and the ADPIs were in full compliance with the limited value stipulated in ANSI/ASHRAE 113-2022.

(3) SV, DeV and IJV can effectively deliver warm air to the occupied zone, with energy saving potential. For MV, more warm supply air was detained in the upper space of the room, resulting in a lower temperature in the occupied zone, and the EUCs values of all cases were not higher than 0.6.

(4) The inhaled air quality in the rooms heated by SV and IJV was better. The ACEs at the breathing zone in all cases of SV and IJV were higher than 1.5. Meanwhile, SV, DeV and IJV showed similar performance on contaminant removal. For MV, the CRE was high when the exhaust outlets were directly above occupants, but the CRE values decreased significantly after changing the location of exhaust outlets.

(5) Compared with MV, the overall score results showed that SV, DeV and IJV had better overall performances in winter. However, it was necessary to avoid too low supply airflow rates for DeV and too high supply airflow rates for IJV. Based on the supply air parameters of this study, DeV and SV were found to have more advantages in heating mode.

Authors' contribution

All authors contributed equally in the preparation of this article.

Declaration of conflicting interests

The author(s) declared no potential conflicts of interest with respect to the research, authorship, and/or publication of this article.

Funding

References

1. Feng X, Liao CH and Cheng Y. Experimental study on the supply air characteristics and thermal comfort of a novel personalized ventilation air terminal device. *Indoor and Built Environment* 2023; 32(6): 1269–1287.

2. Nielsen PV and Xu CW. Multiple airflow patterns in human microenvironment and the influence on short-distance airborne cross-infection – A review. *Indoor and Built Environment* 2022; 31(5): 1161–1175.

3. Liu ZJ, Wang TC, Wang YX, Liu HY, Cao GQ and Tang S. The influence of air supply inlet location on the spatial-temporal distribution of bioaerosol in isolation ward under three mixed ventilation modes. *Energy and Built Environment* 2022; 4(4): 445–457.

4. Cao GY, Kvammen I, Hatten TAS, Zhang YX, Stenstad L, Kiss G and Skogas JG. Experimental measurements of surgical microenvironments in two operating rooms with laminar airflow and mixing ventilation systems. *Energy and Built Environment* 2021; 2(2): 149–156.

5. Ren C, Chen HF, Wang JQ, Feng ZB and Cao SJ. Ventilation impacts on infection risk mitigation, improvement of environmental quality and energy efficiency for subway carriages. *Building and Environment* 2022; 222: 109358.

6. Chen TS, Feng ZB and Cao SJ. The effect of vent inlet aspect ratio and its location on ventilation efficiency. *Indoor and Built Environment* 2019; 29(2): 180–195.

7. Jurelionis A, Stasiuliene L, Prasauskas T and Martuzevicius D. Dispersion of indoor air pollutants emitted at near-floor levels in rooms with floor heating and mixing ventilation. *Indoor and Built Environment* 2018; 27(2): 205–218.

8. Yang B, Melikov AK, Kabanshi A, Zhang C, Bauman FS, Cao GY, Awbi H, Wigö H, Niu JL, Cheong KWD, Tham KW, Sandberg M, Nielsen PV, Kosonen R, Yao RM, Kato S, Sekhar SC, Schiavon S, Karimipanah T, Li XT and Lin Z. A review of advanced air distribution methods-theory, practice, limitations and solutions. *Energy and Buildings* 2019; 202: 109359.

9. Lin Z. Stratum ventilation – A low-carbon way to thermal comfort and indoor air quality. *International Journal of Low-Carbon Technologies* 2017; 12: 323–329.

10. Cheng Y and Lin Z. Experimental investigation into the interaction between the human body and room airflow and its effect on thermal comfort under stratum ventilation. *Indoor Air* 2016; 26: 274–285.

11. Tian L, Lin Z, Wang QW and Liu J. Numerical investigation of indoor aerosol particle dispersion under stratum ventilation and under displacement ventilation. *Indoor and Built Environment* 2009; 18(4): 360–375.

12. Yang B, Liu YH, Liu PJ, Wang FM, Cheng XG and Lv ZH. A novel occupant-centric stratum ventilation system using computer vision: Occupant detection, thermal comfort, air quality, and energy savings. *Building and Environment* 2023; 237: 110332.

13. Cheng FH, Zhang S, Gao SS, Tian X, Liao CH and Cheng Y. Experimental investigation of airflow pattern and turbulence characteristics of stratum ventilation in heating mode. *Building and Environment* 2020; 186: 107339.

14. Zhang Y, Yu WX, Li YL and Li H. Comparative research on the air pollutant prevention and thermal comfort for different types of ventilation. *Indoor and Built Environment* 2021; 30(8): 1092–1105.

15. Zhang S, Lin Z, Ai ZT, Wang FH, Cheng Y and Huan C. Effects of operation parameters on performances of stratum ventilation for heating mode. *Building and Environment* 2019; 148: 55–66.

16. Lin Z, Chow TT and Li Y. Deflection ventilation – A conceptual introduction. In Tham KW, Sekhar C and Cheong D (Eds.), *Proceedings of 7th International Conference Healthy Buildings* 2003; Stallion Press, Singapore, 363–369.

17. Zhang Y, Han O, Li AG, Hou L, Olofsson T, Zhang LH and Lei WJ. Adaptive wall-based attachment ventilation: A comparative study on its effectiveness in airborne infection isolation rooms with negative pressure. *Engineering* 2022; 8: 130–137.

18. Li T, Essah EA, Wu YX, Liao CH and Cheng Y. Numerical comparison of exhaled particle dispersion under different air distributions for winter heating. *Sustainable Cities and Society* 2023; 89: 104342.

19. Haghshenaskashani S and Sajadi B. Evaluation of thermal comfort, IAQ and energy consumption in an impinging jet ventilation (IJV) system with/without ceiling exhaust. *Journal of Building Engineering* 2018; 18: 142–153.

20. Yang B, Liu PJ, Liu YH and Wang FM. Performance evaluation of ductless personalized ventilation combined with impinging jet ventilation. *Applied Thermal Engineering* 2023; 225: 119915.

21. Tan DY, Li BZ, Cheng Y, Liu H and Chen JH. Airflow pattern and performance of wall confluent jets ventilation for heating in a typical office space. *Indoor and Built Environment* 2020; 29(1): 67–83.

22. Ye X, Zhu H, Kang YM and K Zhong. Heating energy consumption of impinging jet ventilation and mixing ventilation in large-height spaces: A comparison study. *Energy and Buildings* 2016; 130: 697–708.

23. Olesen BW, Simone A, KrajcÍik M, Causone F and Carli MD. Experimental study of air distribution and ventilation effectiveness in a room with a combination of different mechanical ventilation and heating/cooling systems. *International Journal of Ventilation* 2011; 9(4): 371–383.

24. Liu H, Wu YX, Li BZ, Cheng Y and Yao RM. Seasonal variation of thermal sensations in residential buildings in the Hot Summer and Cold Winter Zone of China. *Energy and Buildings* 2017; 140(04): 9–18.

25. Jaszczur M, Madejski P, Borowski M and Karch M. Experimental analysis of the air stream generated by square ceiling diffusers to reduce energy consumption and improve thermal comfort. *Heat Transfer Engineering* 2022; 43: 463–473.

26. Lyu JM, Feng X, Cheng Y and Liao CH. Experimental and numerical analysis of air temperature uniformity in occupied zone under stratum ventilation for heating mode. *Journal of Building Engineering* 2021; 43: 103016.

27. Varodompun J and Navvab M. HVAC ventilation strategies: the contribution for thermal comfort, energy efficiency and indoor air quality. *Journal of Green Building* 2007; 2: 131–150.

28. ANSI/ASHRAE Standard 113-2022. *Method of testing for room air diffusion*. American Society of Heating, Refrigerating and Air-Conditioning Engineers, Atlanta, GA, 2022.

29. Rahimi M and Tajbakhsh K. Reducing temperature stratification using heated air recirculation for thermal energy saving. *Energy and Buildings* 2011; 43: 2656–2661.

30. He QB, Niu JL, Gao NP, Zhu T and Wu JZ. CFD study of exhaled droplet transmission between occupants under different ventilation strategies in a typical office room. *Building and Environment* 2011; 46: 397–408.

31. Li XT, Zhao B, Guan P and Ren H. Air supply opening model of ceiling diffusers for numerical simulation of indoor air distribution under actual connected conditions, Part I: Model Development. *Numerical Heat Transfer, Part A: Applications* 2006; 49: 821–830.

32. Blocken B. LES over RANS in building simulation for outdoor and indoor applications: A foregone conclusion? *Building Simulation* 2018; 11: 821–870.

33. Qin C and Lu WZ. Effects of ceiling exhaust location on thermal comfort and age of air in room under impinging jet supply scheme. *Journal of Building Engineering* 2021; 35: 101966.

34. ISO 7730:2005. *Ergonomics of the thermal environment – Analytical determination and interpretation of thermal comfort using calculation of the PMV and PPD indices and local thermal comfort criteria*. The International Organization for Standardization, Geneva, Switzerland, 2005.

35. Cao SJ and Deng HY. Investigation of temperature regulation effects on indoor thermal comfort, air quality, and energy savings toward green residential buildings. *Science and Technology for the Built Environment* 2019; 25: 309–321.

36. Dawe M, Raftery P, Woolley J, Schiavon S and Bauman F. Comparison of mean radiant and air temperatures in mechanically-conditioned commercial buildings from over 200,000 field and laboratory measurements. *Energy and Buildings* 2020; 206: 109582.

37. Huang XY, Luo XL, Shen C, Chang B and Gu ZL. Local heating of a visitor corridor within

a large site museum exhibition hall via an integrated jet ventilation and air curtain system. *Journal of Building Engineering* 2023; 69: 106206.

38. Ren C, Zhu HC and Cao SJ. Ventilation strategies for mitigation of infection disease transmission in an indoor environment: a case study in office. *Buildings* 2022; 12(2): 180.

39. Rehva Guidebook No. 2. *Ventilation Effectiveness*. REHVA: Federation of European Heating and Air-conditioning Associations, Brussels, 2010.

40. Su W, Yang B, Melikov A, Liang CJY, Lu YL, Wang FM, Li AG, Lin Z, Li XT, Cao GY and Kosonen R. Infection probability under different air distribution patterns. *Building and Environment* 2022; 207: 108555.

41. Yamasawa H, Kobayashi T, Yamanaka T, Choi N and Matsuzaki M. Experimental investigation of difference in indoor environment using impinging jet ventilation and displacement ventilation systems. *International Journal of Ventilation* 2022; 21(3): 229–246.

42. Cheng Y and Lin Z. Experimental study of airflow characteristics of stratum ventilation in a multi-occupant room with comparison to mixing ventilation and displacement ventilation. *Indoor Air* 2015; 25: 662–671.

43. Liu J and Lin Z. Energy and exergy analyze of different air distributions in a residential building. *Energy and Buildings* 2021; 233: 110694.

44. Xue K, Cao GY, Liu Meng, Zhang YX, Pedersen C, Mathisen HM, Stenstad LI and Skogas JG. Experimental study on the effect of exhaust airflows on the surgical environment in an operating room with mixing ventilation. *Journal of Building Engineering* 2020; 32: 101837.

45. Qin C, Zhou WR, Fang HQ, Lu WZ and Lee EWM. Optimization of return vent height for stratified air distribution system with impinging jet supply satisfying threshold of |PMV| < 0.5. *Journal of Cleaner Production* 2022; 359: 132033.

46. Serrano-Arellano J, Xamán J and Álvarez G. Optimum ventilation based on the ventilation effectiveness for temperature and CO_2 distribution in ventilated cavities. *International Journal of Heat and Mass Transfer* 2013; 62: 9–21.

47. Ahmed AQ, Gao SA and Kareem AK. A numerical study on the effects of exhaust locations on energy consumption and thermal environment in an office room served by displacement ventilation. *Energy Conversion and Management* 2016; 117: 74–85.

48. He G, Yang X and Srebric J. Removal of contaminants released from room surfaces by displacement and mixing ventilation: modeling and validation. *Indoor Air* 2005; 15: 367–380.

49. Feng GZ, Lei SY, Guo YJ, Meng B and Jiang QF. Optimization and evaluation of ventilation mode in marine data center based on AHP-entropy weight. *Entropy* 2019; 21(8): 796.

50. Cheng FH, Li YH, Wu YX, Cheng Y and Lin Z. Experimental study of air distribution and heating performances of deflection ventilation. *Energy and Buildings* 2023; 282: 112800.

51. Chen HJ, Moshfegh B and Cehlin M. Computational investigation on the factors influencing thermal comfort for impinging jet ventilation. *Building and Environment* 2013; 66: 29–41.

52. Zhang S, Niu D, Li T, Lin Z, Cheng FH and Cheng Y. Cooling effect of air movement on heating performances of advanced air distribution. *Building and Environment* 2022; 226: 109775.

53.   Kong XF, Chang YF, Li NN, Li H and Li W. Comparison study of thermal comfort and energy saving under eight different ventilation modes for space heating. *Building Simulation* 2022; 15: 1323-1337.

54.   Lin Z, Chow TT, Fong KF, Tsang CF and Wang QW. Comparison of performances of displacement and mixing ventilations. Part II: indoor air quality. *International Journal of Refrigeration* 2005; 28(2): 288–305.

55.   Tian X, Zhang S, Awbi HB, Liao CH and Cheng Y. Multi-indicator evaluation on ventilation effectiveness of three ventilation methods: An experimental study. *Building and Environment* 2020; 180: 107015.